NAZARBAYEV UNIVERSITY

School of Engineering and Digital Sciences

Bachelor of Engineering in

Mechanical and Aerospace Engineering

Group 11

The Effect of Nanosized Metal-Organic Frameworks (MOFs) on Fiber Reinforced Polymer

(Final Capstone Project Report)

by

Doszhan Abdygali, Alisher Kabyzhanov, Azat Kassenov

and Zhan Mamytov

Lead-Supervisor: Prof. Sherif A. Gouda

Co-Supervisor: Prof. Gulnur Kalimuldina, Dr. Umut Bakhbergen

April, 2025

Declaration

We, Doszhan Abdygali, Alisher Kabyzhanov, Azat Kassenov, and Zhan Mamytov, hereby declare that this report, entitled “The Effect of Nanosized Metal-Organic Frameworks (MOFs) on Fiber Reinforced Polymer” is the result of our own project work except for quotations and citations which have been duly acknowledged. We also declare that it has not been previously or concurrently submitted for any other degree at Nazarbayev University or elsewhere.

Signature:

Name: Doszhan Abdygali

Date: April 30, 2025

Signature:

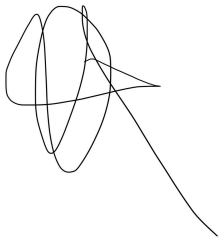

Name: Alisher Kabyzhanov

Date: April 30, 2025

Signature:

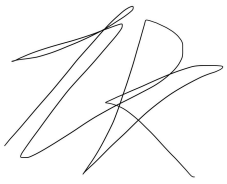

Name: Azat Kassenov

Date: April 30, 2025

Signature:

Name: Zhan Mamytov

Date: April 30, 2025

Acknowledgments

Our team would like to convey our heartfelt thanks to our supervisors, Professor Sherif Gouda and Professor Gulnur Kalimuldina, for their immense support during the whole process of writing the Capstone project, as well as providing us with guidance for each part of the Laboratory practicum. We extend our thanks to Dr. Umut Bakhbergen for her patience and assistance towards our team.

This Capstone Project would not have been properly realized and completed without the support and guidance of each of the superiors.

Abstract

Fiber Reinforced Polymers (FRPs) are a common choice in modern structural manufacture; however, they have mechanical limitations. Metal-organic frameworks (MOFs) are additives whose potential as reinforcement will be explored in this study. During synthesis, cobalt nitrate was used to get MOF called ZIF-67. Scanning electron microscopy (SEM), X-ray Diffraction (XRD), and Fourier Transform Infrared Spectroscopy (FTIR) were used to characterize the obtained powder. After ZIF-67 was incorporated into epoxy matrices at varying weight fractions (0.25wt%, 0.5wt%, 0.75wt%, 1wt%). Composite samples were fabricated with carbon fiber reinforcement and subjected to American Society for Testing and Materials (ASTM) standards. Elastic modulus, flexural strength, and tensile strength were evaluated after testing. Morphological and structural analyses of FRPs were performed using SEM. Extraordinary improvements were achieved in composite with 0.75wt% of ZIF-67. Growth in tensile strength and elastic modulus are reaching up to 14-18%. At higher concentrations, agglomeration occurs and negatively affects the mechanical performance. These results demonstrate the potential of MOF-based composites to improve the mechanical resilience of FRPs. This could be a future option for the aerospace, automotive, and construction industries.

Contents

List of Figures

List of Tables

Chapter I

Introduction

Modern engineering uses more than fifty thousand different materials in various production domains. Those materials could be divided into two different categories: those that were used and known for centuries, and those that developed through technical advancements. This research studies the new material, focusing on composites. Composites became a high-demand material for present engineering, due to their versatility and performance. Such factors made them widely used in aerospace, biomedical, construction and marine sectors [1].

Composite materials are obtained through the consolidation of two or more diverse materials, which follows the emergence of a completely new material with enhanced properties of its components. Typically, composites consist of a matrix and their reinforcement. They are systematized according to the components that were used [2]. This research concentrates on the Fiber-Reinforced Polymers (FRPs), which are a widely used type of composite followed by their optimized strength per unit weight and adaptability to distinct conditions [2].

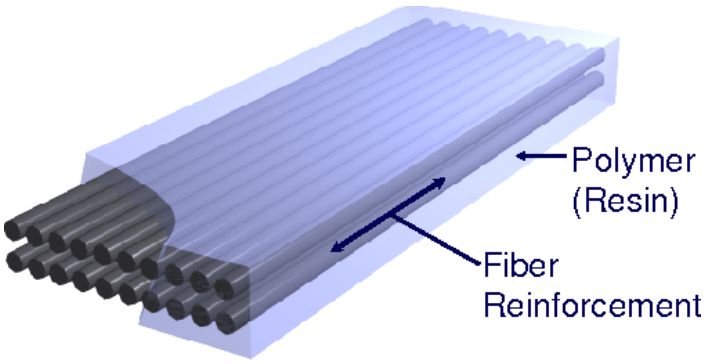

Figure 1.1: Diagram of fiber-reinforced polymer [3].

As shown in Figure 1.1, fiber-reinforced polymers consist of a matrix and fiber reinforcement material. For this research Epoxy resin was utilized as a matrix material for composite. Epoxy is one of the most adaptable, thermosetting polymers applied in adhesives, surface coatings and composites matrices. The tensile and compressive strength of Epoxy are exceptionally high [3]. Also, low shrinkage during curing provides superior dimensional

stability, and outstanding bonding on a wide range of surfaces making it applicable to bonding several materials. Furthermore, epoxy is contrary to some environmental factors, such as chemical and thermal changes, making it durable and reliable for the harshest conditions for aerospace, automotive and construction applications [3].

Carbon fibers are used as fiber reinforcement in research composite, they are thin strands made up predominantly of carbon atoms. This material provides the advantages of being both lightweight and having high strength, which makes them optimal materials across various industries [2]. Such a combination further enhances the tolerance of heat, while reducing the weight. More importantly, the carbon fibers do not fatigue or wear out easily; hence, being very durable for extreme use applications [2].

Aside from reinforcement and matrix, there are specific roles for additives in FRPs. Different materials are generally mixed with the composite to achieve specific characteristics that would be applied to a desired application. To make a contribution to material properties, additives and filters are generally added in small quantities into fiber-reinforced polymers, often no more than 1-2 wt% [3]. Based on the chemicals, additives commonly used to enhance stability, flame retardancy and UV absorption: flame retardants reduce the flammability of the material, ultraviolet (UV) absorbers help materials resist degradation caused by sunlight, colorants and anti-static agents are used to improve aesthetics or functionality. Others are more process-friendly, such as reducing cure time or improving flow characteristics during processing. Briefly stated, FRP additives play the dual function of performance and toughness enhancement as well as meeting some needs of industries [2].

Beyond traditional additives, there are recently discovered advanced materials like Metal-Organic Frameworks (MOFs) are being introduced into composites. MOFs are a group of materials which became in demand because of their interesting structure and adjustable properties. As shown in Figure 1.2, MOFs are metal clusters or ions guided by organic ligands to assemble a porous crystalline framework [3]. Due to their chemical and thermal stability properties, such characteristics allow them to be applied in different fields, including gas storage, catalysis, or drug delivery. Such capabilities can facilitate the customization of the interaction of MOFs with the medium, leading to the synthesis of efficient adsorbents, catalytic, and reinforcement systems in composite media.

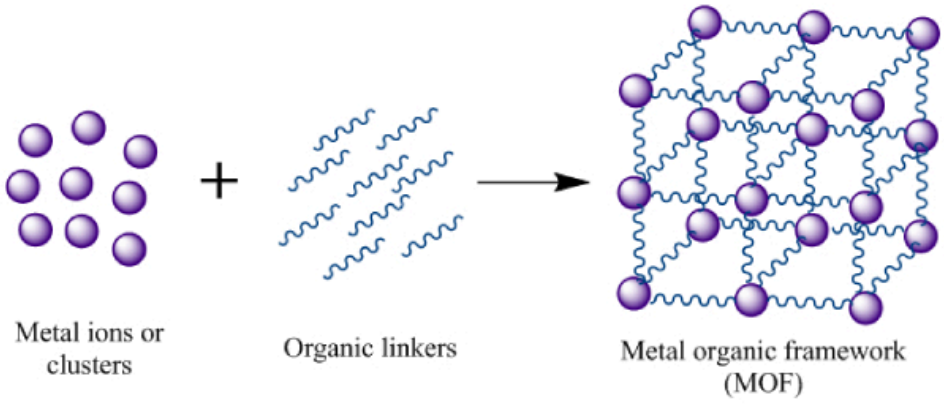

Figure 1.2: Structure of MOFs [3]

Extensive porosity of MOFs leads to substantial surface area, which improves unique gas storage characteristics (e.g., hydrogen or carbon dioxide storage characteristics). Also, tunable chemical structure of MOFs makes selective gas separation possible (e.g, natural gas separation and carbon sequestration) [3]. High thermal and mechanical stability also develops their ability to withstand extreme conditions. MOFs inclusion to composites also increase their mechanical, thermal and environmental stability. Some groups of MOFs could be used as multi-functional materials that can integrate electric conductivity, magnetic properties and catalytic activity [4].

This research focuses on Zeolitic Imidazolate Frameworks (ZIFs). They are MOFs which belong in a zeolite topology that focus on improving durability on a wide temperature range and reactive environments. ZIF-8 and ZIF-67, which are made of zinc and cobalt ions respectively. They are especially distinguished for their high stability and large surface area. Therefore, ZIFs have prodigious potential for the reinforcement of polymer matrices and multifunctional advanced composites. Structure of ZIF-67 shown in Figure 1.3. The compound is added to epoxy resin, which is known for proven mechanical strength and natural resistance, hence it offers significant potential for the preparation and development of composites with upgraded properties [4].

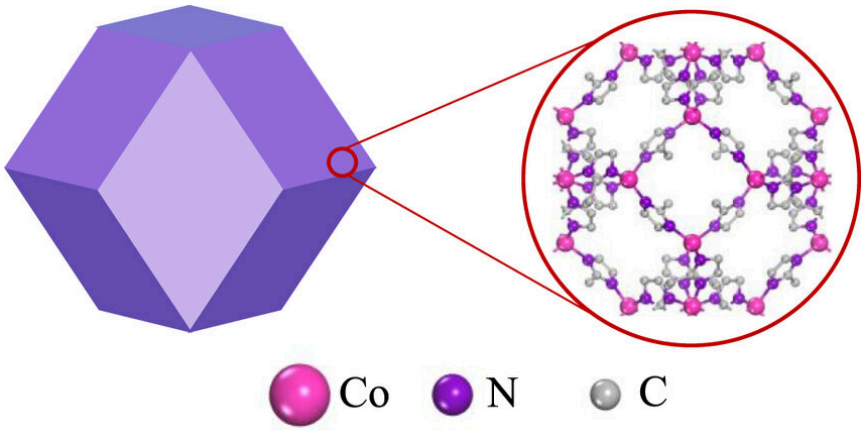

Figure 1.3: The ZIF-67 structure. [4].

This study is relevant for further contributions to elaborating high-performance, multifunctional composite materials into application. Corresponding improvements create a new path toward the advancement of more high-strength and durable materials operating under extreme conditions [2]. Obtained results with the context of the present work could create interest to industries dealing with high thermal and mechanical stresses, like aerospace, automobile and defense. Apart from that, MOFs could be applied not only for thermal stability, enhancement of mechanical properties, or environmental conditions, but also have potential in composite materials in the future [4].

In this research, metal-organic frameworks (MOFs) have a vital role in strengthening the mechanical characteristics of FRP. Therefore, with the addition of nanosized ZIF-67 as filler material in epoxy resin, the study's goal is to overcome the mechanical limitations associated with traditional FRP and thereby manufacture composites with improved properties.

Table 1.1: Task Description & Distribution between team members

Team Member	**Capstone Project Involvement**
Doszhan Abdygali	Literature review, Preparation of Fiber-Reinforced polymers, Preparation of Metal-Organic Frameworks
Alisher Kabyzhanov	Literature review, Preparation of Metal-Organic Frameworks, Tensile and Three-Point Bending Tests, Data Analysis.
Azat Kassenov	Literature review, Preparation of Fiber-Reinforced polymers, Data Analysis.
Zhan Mamytov	Literature review, Preparation of Metal-Organic Frameworks, Characterization, Data Analysis.

Chapter II

Literature review

2.1 FRP Analysis

Fiber Reinforced Polymers (FRPs) are composite materials consisting of a polymer matrix reinforced with fibers that have revolutionized structural engineering; tensile strength, superior corrosion resistance properties of FRPs make them indispensable in aerospace, automotive, and civil engineering [5]. High strength-weight ratio and superior stiffness of carbon fiber-reinforced polymers (CFRPs) make them appropriate for most aerospace, military, and civilian applications [1]. The inert surface of carbon fibers (CFs) often leads to weak fiber-polymer interfacial adhesion, limiting the mechanical performance. The interface, a critical region where load transfer occurs between fibres and the matrix, determines composite's overall strength and toughness [2].

To improve the interfacial properties, polar groups have been introduced to bond more effectively and improve wettability with resin [5],[7]. Covalent (formation of bridge) and non-covalent (van der Waals forces) influence enhance the adhesion without affecting CF tensile strength significantly [8]. Asbestos removal and surface modifications (oxidation, plasma treatment, chemical grafting) are encouraging techniques for forming a transition layer to minimize stress concentrations and improve load transfer [9],[10]. For example, the deposition of CNTs on CF surfaces via chemical vapor deposition significantly increased the interfacial bonding strength [13].

Increased adhesion contributes to better mechanical properties, but too much strength at the interface makes it brittle, and crack propagation occurs quickly under stress. Future investigations will undoubtedly target interface toughening and novel multi-scale modification strategies as a means for balancing these complementary properties [5].

2.2 Challenges in FRPs

According to Bibekananda and Bera**,** the most common challenges of the application of Fiber Reinforced Polymers (FRP) are related to interfacial debonding and low resistance to mechanical stresses such as tensile and flexural loads. Poor adhesion reduces composites' ability to transfer stress effectively between matrix and fibers, consequently causing premature failure [6]. Figure 2.1. demonstrates the morphology of the fiber-matrix interface.

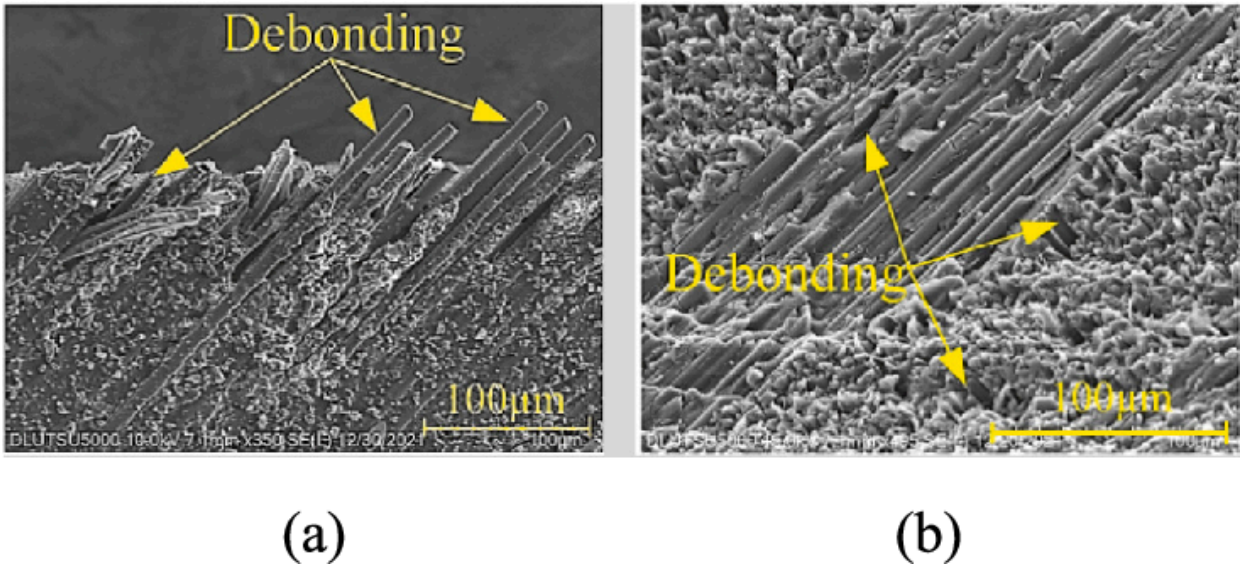

Figure 2.1: Fiber-Matrix Interfacial Debonding (a) Burrs due to debonding. (b) Fiber pull-out due to debonding [9].

In addition to interfacial debonding, mechanical challenges in FRPs are often related to the following:

1. **Stress Concentration and Agglomeration Issues**:

   For FRPs, a uniform distribution of reinforcements like MOFs or fibers is needed to carry the load without failure. This clustering leads to stress concentrating defects, poor dispersion. They are resulting in reduced tensile and flexural strength. As an example, this can decrease tensile strength by up to 30% in randomly dispersed reinforcements; this value is compared to uniformly dispersed systems [8]. This issue can be solved using advanced mixing techniques such as ultrasonic dispersion [6], resulting in a considerable

improvement in tensile strength, which has been emphasized by a 27.2% increase using sonication [8].

2. **Fiber-Matrix Interface Weakness**:

   During the application of mechanical stress, usually captured by phenomena of fiber pull-out and cracking in matrix, which deeply diminishes the load-bearing capacity. Insufficient bonding hinders successful stress transfer, leading to mechanical failure at early stages. Surface modifications, like alkali treatment, can increase tensile strength (by 36%) and Young's modulus (by 53%), thus overcoming interfacial weakness [10].

3. **Delamination**:

   One of the vital mechanical problems of FRPs is the delamination under cyclic or impact loading, despite the advances in FRPs. In your composite, it is due to poor adhesion between the layers, leading to crack propagation between the layers of the composite. The use of silane-treated fibers is shown to reduce the delaminations significantly, with an improvement of 38% in flexural modulus, guaranteeing sufficient bonding between layers [10].

2.3 Role of Nanomaterials in FRPs

The failure of FRPs in their applications led to an enormous amount of research, mainly focused on finding a way to enhance their mechanical properties. Common solution was the manipulation of FRP in terms of fiber orientation and materials for each layer. The research conducted by Darain K. and Zia A., claims that the addition of CFRP laminates significantly increases strength and durability of the supports [8]. However, such methods were not appropriate in terms of cost and manufacturing process. The research conducted by Khan et al.**,** analyzed influence of incorporating inorganic oxide aerogels into SiO_2, Al_2O_3, and ZrO_2 composites and highlighted an enormous improvement in terms of temperature stability, processability, and shape formation [29]**.** Another approach involved the utilization of nano-sized materials as fillers, due to their remarkable ability to create a strong link between fibers and the matrix, which consequently ensures effective stress transfer. According to Rashid et al, such compositions are more durable and strong in contrast to traditional materials in the

defense sector [3]. Maske and Demiroglu, analyzed mixture of various nanoparticles in glass fiber composites and reported that incorporation of carbon nanotubes significantly boosted not only the tensile and flexural strength of the final product but also improved flame retardancy and water absorption ability [10], [31]. Another research suggests that the addition of cellulose nanocrystals into composites creates a unique product with enhanced chemical and physical properties [15].

Therefore, several reports concluded that the most optimal and effective in terms of cost solution to Interfacial Debonding and poor mechanical properties of FRPs is the addition of nanomaterials [16], [17]. Table 2.1 demonstrates the results of different studies that utilized Carbon Fiber Epoxy as the main FRP system and different types of nanofillers for the enhancement of mechanical properties.

Table 2.1: Improvements after adding different nanofillers into Carbon fiber-epoxy

FRP system:	**Type of nanofiller:**	**Fabrication process:**	**Improvement of mechanical properties:**	**Reference:**
Carbon fiber-epoxy	Silane-modified nano-clay	Slurry compounding and wet lay-up	Storage modulus: 40 %; Flexural modulus: 24 %; Tensile modulus: 16 %;	[18]
Carbon fiber-epoxy	Carbon nanotube	Vacuum-assisted resin transfer moulding	Flexural strength: 18 %; Flexural modulus: 11.6 %	[19]
Carbon fiber-epoxy	Silane-modified carbon nanotubes	Hand lay-up	Tensile strength: 15.8 %; Elastic modulus: 18 %	[20]
Carbon fiber-epoxy	Carbon nanotube	Vacuum-assisted resin transfer moulding	Tensile strength: 18 %; Stiffness: 24 %	[21]
Carbon fiber-epoxy	Carbon nanofiber	Vacuum-assisted resin infusion method	Compressive strength: 19.8 %;	[22]

Carbon fiber-epoxy	Graphene oxide	Autoclave	IFSS: 35 %; ILSS: 12.7 %	[23]
Carbon fiber-epoxy	Graphene nano-platelets	Hand lay-up and autoclave	Flexural strength: 82 %; ILSS: 19 %	[24]

2.4 Improvements of Mechanical properties by MOFs

MOFs are arguably the most promising among all accessible nanoparticles. Duan et al. asserted that NOFs have the unique ability to offer a higher level of chemical and structural tunability than all other types of nanofillers. MOFs can be designed to have particular properties as a result of mixture of metal nodes and organic joints [25]. In addition, MOFs have an exceptionally large surface area and porosity, enabling better interaction with the polymer matrix, which consequently can lead to improved stress transfer, interfacial bonding, and energy dissipation, reducing crack propagation around stress concentrators [26]. A.B. Rashid and M. Haque believe that with extensive surface area, variable porosity, and the capability of incorporating different functional groups, they can be considered good candidates for the improvement of FRP composites [9].

The combination of MOFs with matrix composites has proved to provide dramatic improvements in mechanical properties. For instance, Ayyagari et al. showed that composites modified with MOFs presented an enhancement of 11% on tensile strength when compared to unmodified fibers, as a consequence of an enhanced load transfer in matrix [22]. Consistent with that, the shear lap joint strength of MOF composites increased by the amount of 40%, which was ascribed to mechanical interlocking and extended bonding surface areas provided by the porous MOF structures [22]. The results of both analysis summarized in Figures 2.2 and 2.3. Moreover, incorporation of MOFs noticeably improved both flexural strength and modulus , also MOFs significantly decreased the propagation of microcracks and enhanced the load-carrying capacity [29]. MOFs additionally gave a remarkable rise in the damping parameter of 700%, indicating better interfacial adhesion and energy dissipation [30].

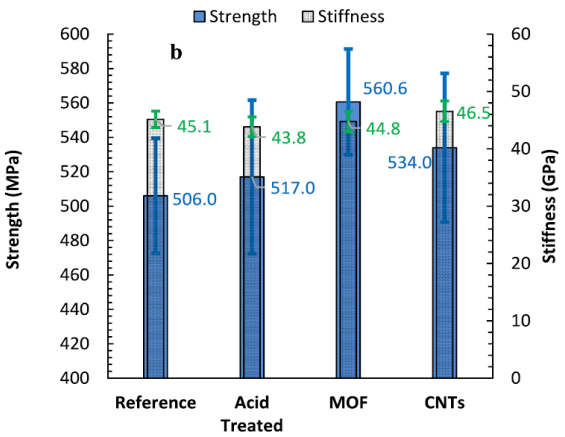

Figure 2.2: Results of Tensile testing [22]

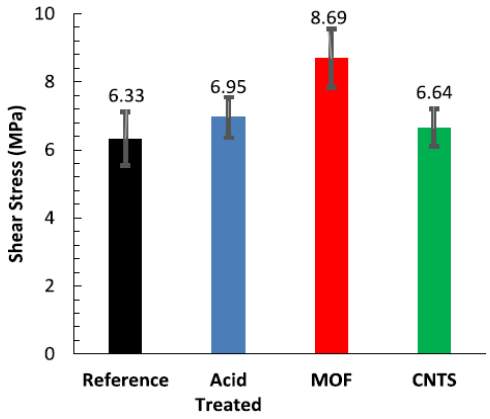

Figure 2.3: Results of Shear Lap Joint Strength testing [22]

Within the broad category of MOFs, certain types have demonstrated particular efficacy in composite reinforcement:

- **ZIF-8**: Structurally, ZIF-8 is a zeolitic imidazolate framework that has been extensively investigated for its relative stability and large surface area. Zhang et al., found a 31% increase in compressive strength when incorporating ZIF-8 in Portland cement composites, which was due to ZIF-8 acting as a nucleation site during hydration [15]. For example, ZIF-8 effectively enhances the wear resistance of fabric composites by creating a uniform transfer film that can facilitate interfacial bonding [20].
- **TiN@ZIF-8 Hybrid**: Zhang et al., prepared a titanium nitride-ZIF-8 hybrid that realized a 48% enhancement in the tensile strength of fabric composites. The hybrid system offered better thermal resistance and mechanical stability compared to its monolithic counterparts, indicating a possible synergistic effect between the TiN and ZIF-8 [20].
- **General MOFs**: Across multiple studies, the incorporation of MOFs has been consistently associated with improvements in shear lap joint strength and damping capacity, making them valuable for applications requiring high durability and dynamic stress resistance [27], [28].

Table 2.2: Analysis of enhancement of FRPs after and before the addition of ZIF-8, TiN@ZIF-8 Hybrid, and general MOFs

MOF Type	Property	Untreated Composite	MOF-Treated Composite	Improvement %
ZIF-8	Compressive Strength	40 MPa	52.4 MPa	+31%
TiN@ZIF-8 Hybrid	Tensile Strength	200 MPa	296 MPa	+48%
General MOFs	Shear Lap Joint Strength	200 MPa	280 MPa	+40%
General MOFs	Damping Parameter	0.05	0.35	+700%

The substantially improved performance of MOF-modified composites is attributed to several important mechanisms:

1. **High Surface Area and Porosity**: MOFs provide extensive surface-area, that enhances not only fiber-matrix interactions and stress transfer between fiber but also matrix and load distribution [17], [18].
2. **Interfacial Bonding**: Functional groups on MOF surfaces facilitate chemical bonding with polymer matrices, improving adhesion and reducing delamination risks [19], [22].
3. **Energy Dissipation**: The high damping capacity of MOFs, particularly in dynamic environments, leads to reduced impact of vibrational stresses and also extends the lifespan of composites [19].

2.5 Fabrication

Incorporation of MOFs into FRPs could be challenging as there are several requirements such as even dispersion of nanoparticles in the polymer. Further, there needs to be solid interfacial bonding between MOFs and fibers. Some general approaches for incorporation include:

1. **Direct Dispersion:** MOFs are introduced straight into the polymer matrix before composite preparation. Although simple, this approach needs to be precisely controlled to avoid agglomeration that may reduce the mechanical properties of the FRPs. Al-Haik et al. highlighted a 76.8% improvement in the elastic modulus at 0.5 wt. % filler concentration in terms of pure epoxy, which represents the promising potential, but with a lot of work to be done [23].
2. **Surface Modification of Fibers**: The MOFs can be cut via chemicals or physically on the surface of reinforcing carbon, which greatly improves the adhesion between faces. This technique is highly useful in enhancing shear strength and preventing delamination upon mechanical loading. Treated composites were 36% higher than for untreated composites in terms of tensile strength (e.g,. alkali-treated sisal fiber composites). Likewise, the tensile strength of silane-cured composites (76 MPa) was significantly larger in contrast to corresponding value for untreated composites (67 MPa) [24], underlining the role of nanofiller in improving mechanical properties through surface modification.
3. **In-Situ Polymerization**: MOFs are added during polymerization of the matrix material itself, which leads to better control of their distribution and orientation. It may yield more uniform properties across the composite, but it is more complicated and labor-intensive.

Chapter III

Methods & Materials

3.1 Design of Experiments

The experimental design was aimed at evaluating the impact of nanosized Metal-Organic Frameworks (MOFs), specifically ZIF-67, on mechanical characteristics of fiber-reinforced polymers (FRPs). Tensile, flexural strengths and elastic modulus measurements were found by the quantitative approach applied following ASTM standards. The experiment was carefully planned and performed according to the following stages:

1. ZIF-67 MOF Synthesis:

The solvothermal technique was used to synthesize ZIF-67, enabling strict control over temperature, time, and reactant ratios to achieve homogeneous particle formation. Optimization of these parameters was attempted for reproducible distribution and uniform particle sizes.

2. Fabrication of Composite Samples:

ZIF-67 particles were distributed homogeneously inside the matrix at certain weight percentages to prepare composite specimens (0.25%, 0.50%, 0.75%, 1.00%). Then the specimens were cut into laminates following ASTM standards for consistency and reproducibility.

3. Testing and Analysis:

Mechanical tensile and flexural characterization were performed alongside characterization techniques such as XRD for structural analysis, SEM for morphological analysis, and FTIR for chemical bond confirmation. The data obtained was compared with existing literature for result validation.

4. Reporting and Interpretation:

The results were presented in graphical representations such as graphs and SEM images, then analyzed with respect to available theoretical backgrounds in order to develop coherent conclusions about the material behavior.

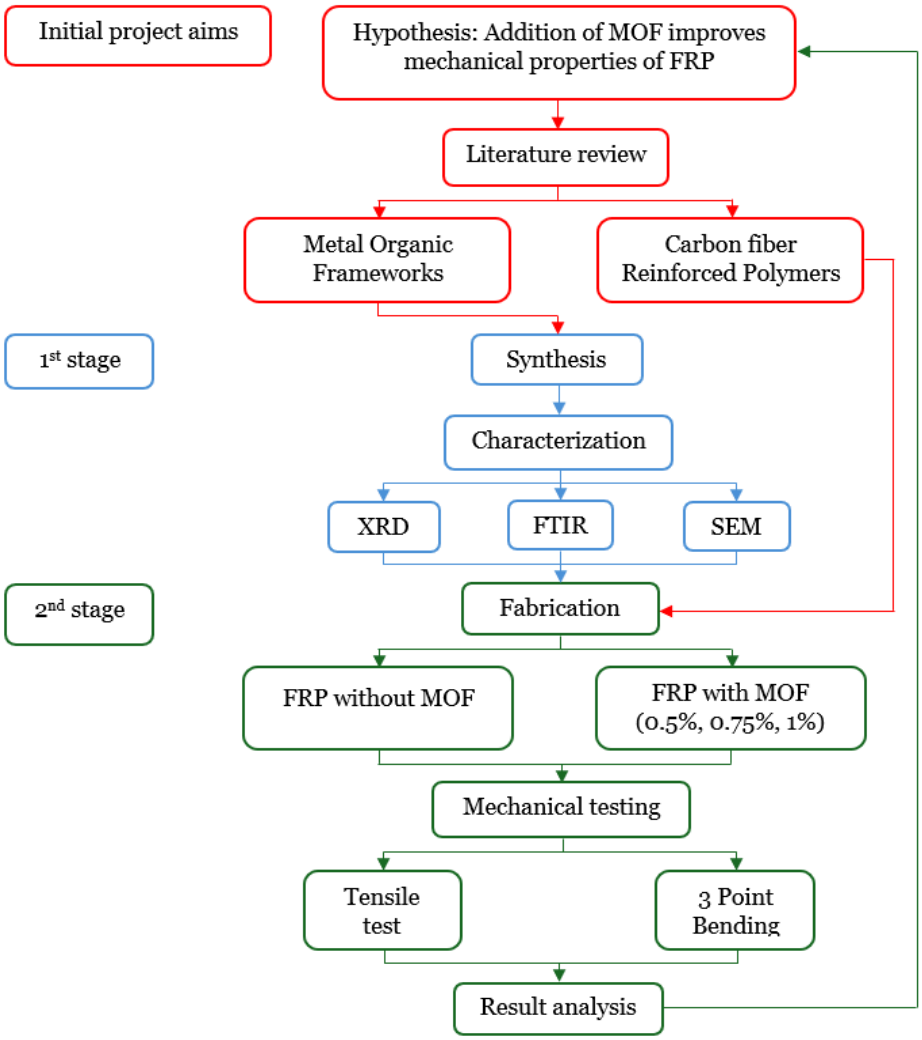

Figure 3.1: Project flowchart.

The principal hypothesis of this research was that integration of ZIF-67 into an epoxy would develop the mechanical aspects of FRP through enhanced fiber-matrix interaction. The specific goals of this study were:

- Analysis of the impact of MOF concentration in terms of flexural and tensile properties.
- Analysis of SEM micrographs in terms of bonding behavior and particle dispersion.

- Conduction of XRD to analyze crystalline phases and structural characteristics of ZIF-67.
- Performing FTIR testing to validate functional groups and assure chemical bonding.
- Identifying possible problems, such as particle agglomeration and interface failure.

A coding system was introduced to differentiate samples based on MOF concentration and test type. For instance, "T0.25" refers to a tensile test sample with 0.25% concentration. This method simplified data collection and analysis and reduced the possibility of procedural errors.

Table 3.1: Codes Table

Code	Description
REF	Reference sample without ZIF-67
T0.25	Tensile specimen with 0.25% ZIF-67 concentration
T0.50	Tensile specimen with 0.50% ZIF-67 concentration
T0.75	Tensile specimen with 0.75% ZIF-67 concentration
T1.00	Tensile specimen with 1.00% ZIF-67 concentration
F0.25	Flexural specimen with 0.25% ZIF-67 concentration
F0.50	Flexural specimen with 0.50% ZIF-67 concentration
F0.75	Flexural specimen with 0.75% ZIF-67 concentration
F1.00	Flexural specimen with 1.00% ZIF-67 concentration

Furthermore, various strategies were implemented in order to minimize the impact of potential sources of error. These strategies consisted of optimization of stirring time during the synthesis process, utilization of vacuum degassing to remove air bubbles, and analysis of uniform fiber alignment throughout the laminate manufacturing process.

The experimental procedure was planned to achieve reproducible and consistent data that would be highly comparable with the existing research. The systematic procedure guaranteed transparency and that each phase presented important information about the FRP composite material behavior with ZIF-67 MOFs.

Table 3.2: Project work Gantt chart

Task name	September	October	November	December	January	February	March	April
Literature review								
ZIF-67 Synthesis								
Characterization (XRD, SEM, FTIR)								
FRP Fabrication								
Mechanical Testings								
Data analysis								

3.2 Materials and Equipment

3.2.1 Materials

1. 2-Methylimidazole ($C_4H_6N_2$): 0.66 g (Sigma-Aldrich, 99% purity);
2. Cobalt(II) Nitrate Hexahydrate ($Co(NO_3)_2 \cdot 6H_2O$): 0.46 g (Sigma-Aldrich, 98% purity);
3. Methanol (CH_3OH): 30 mL (analytical grade);
4. Epoxy Resin (Bisphenol A-based): 1 kg;
5. Carbon Fiber (Unidirectional, 2.5 mm thick): 310 mm × 270 mm sheets.

3.2.2 Equipment

1. Magnetic Stirrer (IKA RCT Basic): For solution preparation;
2. Centrifuge (Hettich Rotina 420): Capable of 7000 rpm;
3. Vacuum Drying Furnace (Memmert VO): Temperature range 60–80°C;
4. X-ray Diffraction (XRD) (Rigaku MiniFlex 600): For crystal structure verification;
5. Fourier Transform Infrared Spectroscopy (FTIR): For chemical structure descriprion;
6. Scanning Electron Microscope (SEM): For morphological observations;
7. Water Jet Cutter: For precise cutting of fiber sheets;
8. Universal Testing Machine (Instron 5967): For tensile and flexural testing.
9. HEWXWX Ultrasonic Cleaner;
10. Single-Stage Vacuum Air Pump Single Stage Vacuum Pump for 1L vacuum suction filtration used in lab; AMEERR

3.3 MOF Synthesis Procedure

Step 1: Solution Preparation

1) 0.46 g of $Co(NO_3)_2 \cdot 6H_2O$ and 0.66 g of $C_4H_6N_2$ were placed in a 50 mL glass beaker.
2) 30 mL of methanol was added to dissolve the content of the beaker.
3) The mixture was mixed under magnetic stirring at room temperature (20–25°C) for 24 hours.

Step 2: Precipitation and Washing

1) The obtained suspension put on a centrifuge at 7000 rpm for 5 minutes to separate the ZIF-67 precipitate.
2) For better purity of ZIF-67, the sediment was washed with 10-15 mL of methanol three times.

Step 3: Drying and Storage

1) The purified ZIF-67 was inserted to dry in a vacuum furnace at 70°C for 24 hours.
2) Dried powder was stored in a desiccator to prevent moisture absorption.

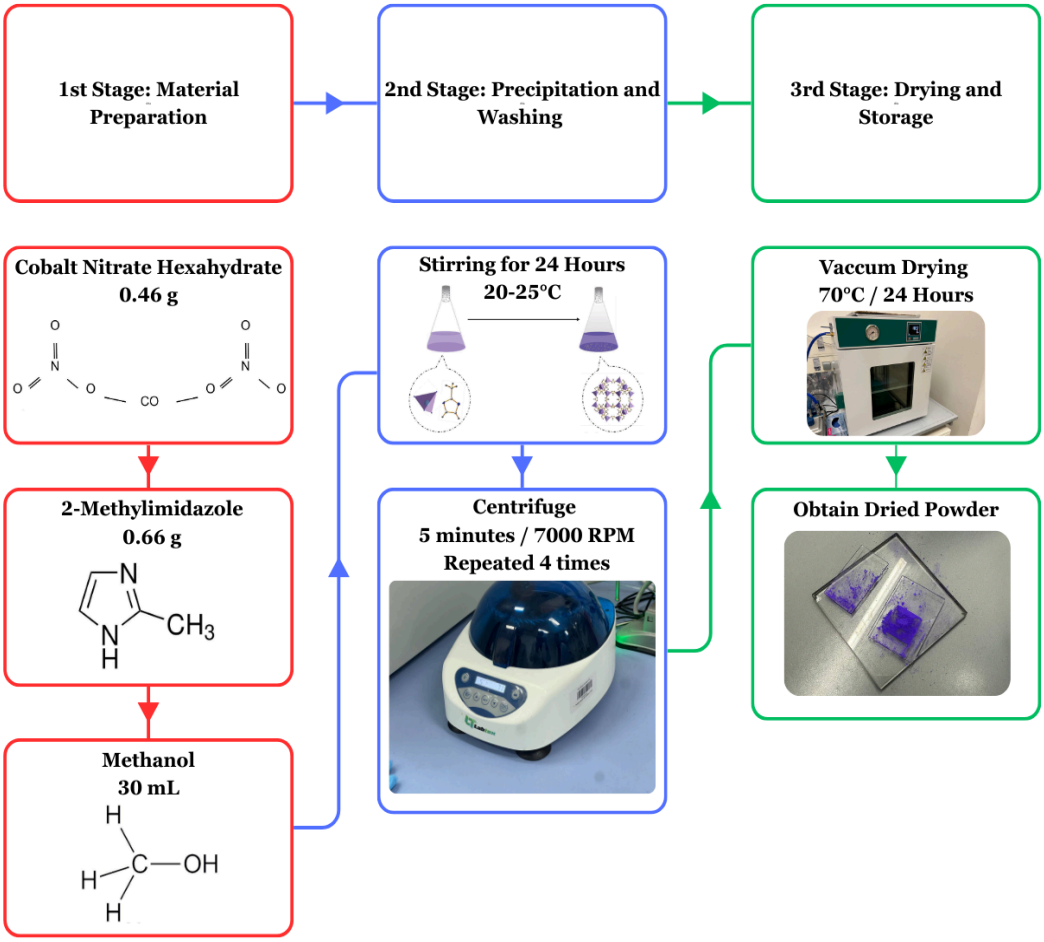

Figure 3.2: Synthesis Process Diagram

3.4 Composite Fabrication

Step 1: Epoxy-MOF Mixing

1) Prepare 31.32 grams of epoxy resin and 8.7 grams of hardener.
2) ZIF-67 was mixed into the hardener at the following weight fractions: 0.25%, 0.50%, 0.75%, and 1.00%. Hardener with ZIF-67 stirred by hand for 10 minutes.
3) Mixture ultrasonicated for 15 minutes, for unifying ZIF and hardener

4) Hardener with ZIF-67 hand mixed with Epoxy resin for 10 minutes.
5) Mixture ultrasonicated in an ice bath for preventing early curing.
6) The mixture degasses under vacuum for 30 minutes to prevent void formation.

Step 2: Laminate Assembly

1) The epoxy-MOF mixture was manually applied to carbon fiber layers using the hand lay-up technique.
2) Additional layers for vacuum bagging applied on the top of the prepared mold. Breather fabric, peel ply, perforated release film, release film.
3) A vacuum bagging process was applied for 72 hours.

Step 3: Fiber Preparation

1) Carbon fiber sheets were cut using a water jet cutter to dimensions specified by ASTM D3039 (tensile) [32], and ASTM D790 (flexural) [33].

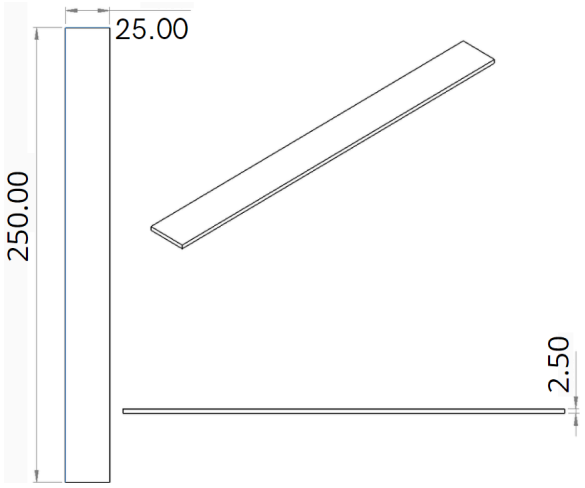

Figure 3.3: Test specimens dimensions for Tensile testing

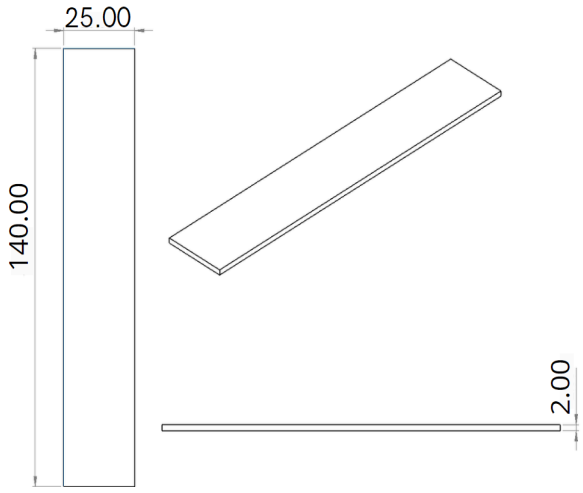

Figure 3.4: Test specimens dimensions for Flexural (3 Point-Bending) testing

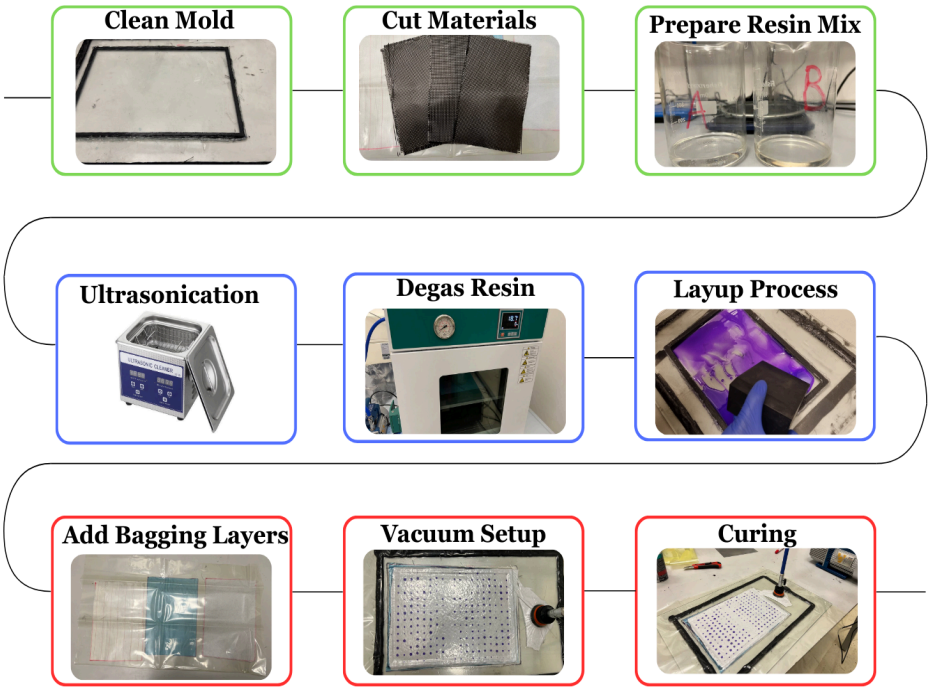

Figure 3.5: Composite Fabrication Process

3.5 Testing Procedures

3.5.1 Tensile Testing

Tensile strength and elastic modulus were measured on an Instron 5967 machine according to ASTM D3039 standards. Size of 250 mm × 25 mm × 2.5 mm specimens are prepared to obtain accurate and even mechanical properties measurements.

3.5.2 Flexural Testing

Flexural modulus and strength measurements were recorded according to the ASTM D790 test standards. The specimens of 140 mm × 25 mm × 2 mm were subjected to a three-point bending test for defining their flexural behavior and mechanical response when subjected to an applied load.

Figure 3.6: Universal testing machine (Instron 5967)

3.5.3 Morphological Analysis

Morphological characterization was done through SEM imaging to explore the dispersion of ZIF-67 in epoxy matrix and the fiber-matrix structure. XRD analysis confirmed crystallinity of the MOfs synthesized, while FTIR spectroscopy confirmed the chemical bonds and functional groups within the composite for complete characterization of the materials used.

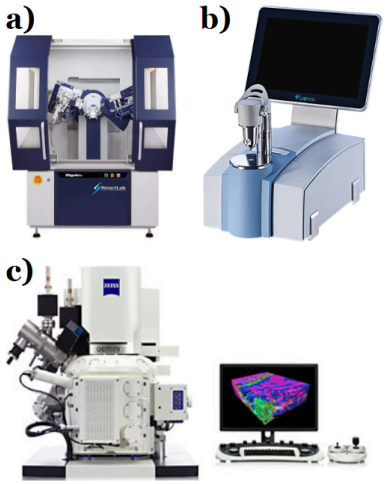

Figure 3.7: (a) XRD machine, (b) FTIR machine, (c) SEM machine.

Chapter IV

Results and Discussion

4.1 Structural and Morphological Characterization of ZIF-67 Nanoparticles

4.1.1 X-ray Diffraction (XRD) Analysis

The X-ray diffraction (XRD) was performed to confirm both phase purity and structural integrity of the crystallographic properties of the synthesized ZIF-67. In Figure 4.1, sharp diffraction peaks correspond to the characteristic reflections of ZIF-67's sodalite-like crystalline structure (at 7.5°, 10.5°, 12.9°, 14.9°, 16.6°, 18.2°, 22.3°, 24.6°, 25.8°, and 26.8°, in correspondence to the crystal planes (011), (002), (112), (022), (013), (222), (114), (134)). After comparing the obtained results with the reviewed literature, it was found that all peaks align with references [14]. Such results suggest that the obtained product is a highly crystalline material.

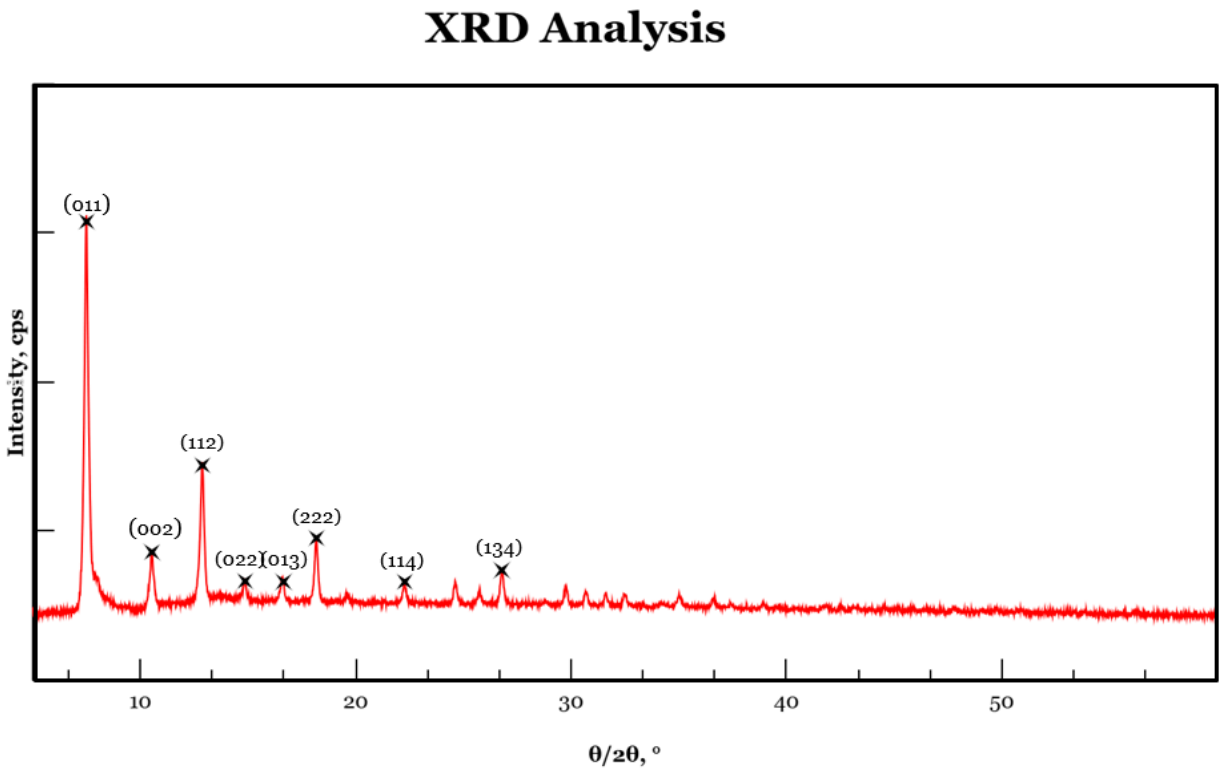

Figure 4.1: XRD graph

Moreover, the absence of impurity peaks indicates that the synthesis process was performed successfully and the parameters of the reactions were correctly controlled. The sharpness and intensity of the peaks indicate the material's stability and confirm functional properties of the product. After comparison with similar studies [15], [16], [17], it was confirmed that the obtained ZIF-67 nanoparticles had superior degree of crystallinity, which also indicate that the reaction conditions were optimized correctly.

4.1.2 Scanning Electron Microscopy (SEM) Analysis

Scanning Electron Microscopy (SEM) was utilized in order to determine the morphology of nanoparticles of ZIF-67, which were synthesized during the laboratory practicum. Obtained microscopy images (Figure 4.2) validate that the process of ZIF-67 synthesizing was done correctly. Having a rhombic dodecahedral structure is expected to be the common characteristic of ZIF-67 [15]. Well-defined edges as well as minimal surface defects are being clearly observed via microscopy images. Moreover, the most important validation made via Scanning Electron Microscopy with high-magnification parameter, is presence of densely packed nanoparticles, which in turn propose the chance of minimum agglomeration occurring. Therefore, combining both of the validations, the successful synthesis process of ZIF-67 is expected to be drawn.

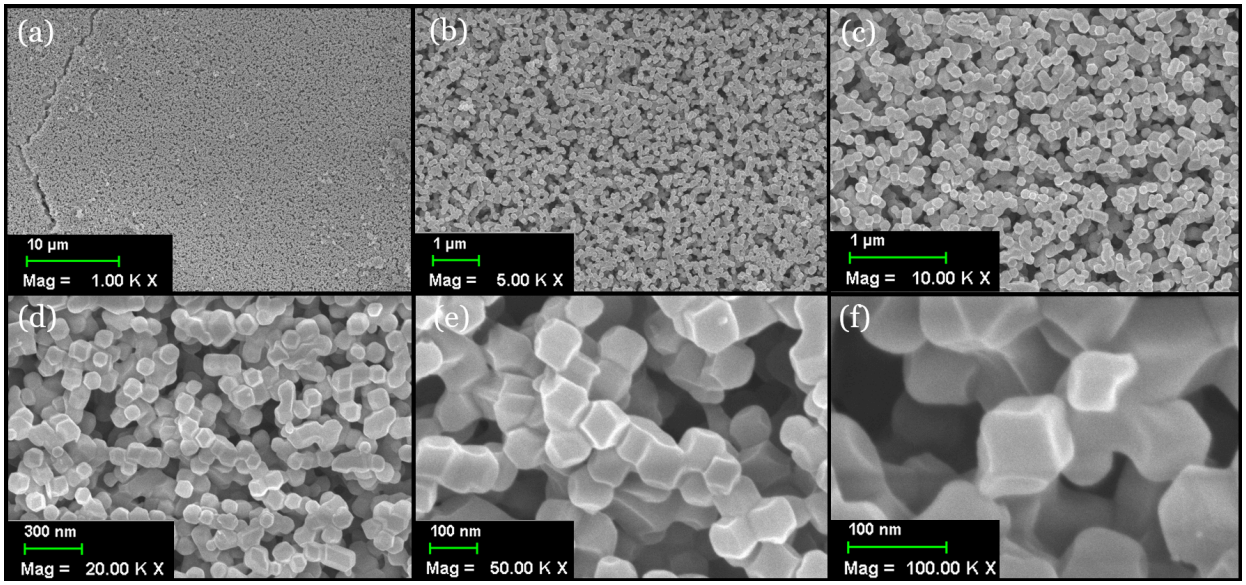

Figure 4.2: SEM Images of ZIF-67

4.1.3 Fourier-transform infrared spectroscopy (FTIR) Analysis

FTIR analysis was performed in order to check bonds and functional groups on surface. Figure 4.3 illustrates the FTIR spectrum of the ZIF-67 nanostructure. The results lie in the adsorption span of 400-4000 cm^{-1}. The peaks at 3360 cm^{-1} and 1360 cm^{-1} indicate C–H bond in imidazole, while the peak at 1750 cm^{-1} corresponds to the C=H bond. In addition, the peak at 420 cm^{-1} shows the existence of Co–N bond. The comparison with similar studies confirmed the characteristics of the obtained ZIF-67 [25].

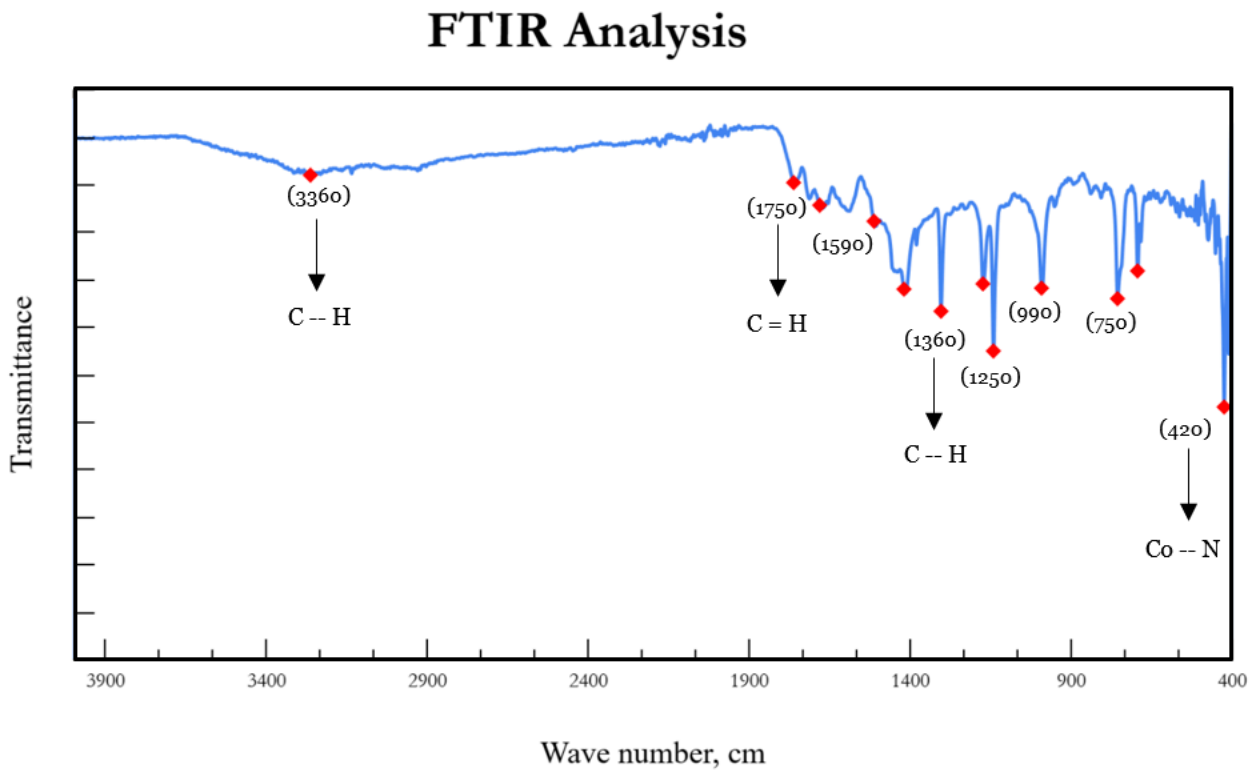

Figure 4.3: FTIR graph

4.2 Mechanical testings

4.2.1 Tensile testing

Tensile test was conducted for various concentrations of ZIF-67. The research was done for concentrations 0.0%wt, 0.25%wt, 0.5%wt, 0.75%wt, and 1.0%wt. Figure 4.4 shows Stress-strain graphs, while Figure 4.5 demonstrates an overall comparison of average values

between them. It was observed that the sample with 0.75%wt has achieved the highest tensile strength (342MPa) and the second highest result corresponding to 0.5%wt (309MPa).

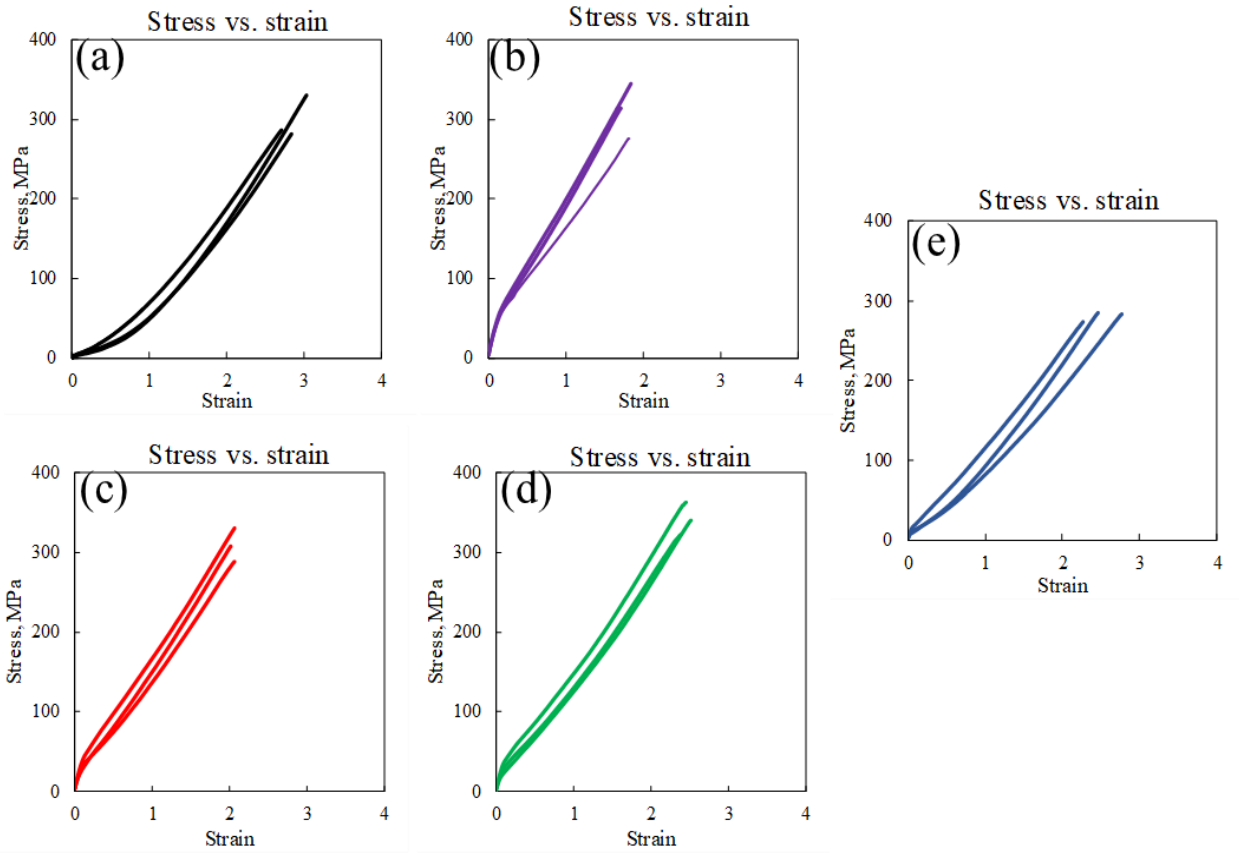

Figure 4.4: Tensile Tests for FRP with different MOF fractions: (a) 0%wt, (b) 0.25%wt, (c) 0.5%wt, (d) 0.75%wt, and (e) 1%wt.

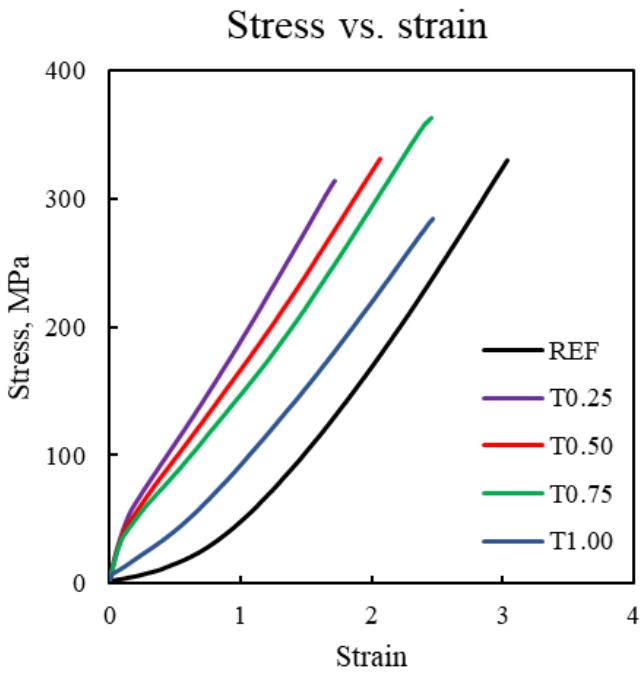

Figure 4.5: Tensile Tests for FRP with different MOF fractions

Figure 4.6 demonstrates average Tensile strength for concentrations 0%wt, 0.25%wt, 0.5%wt, 0.75%wt, and 1.0%wt. They also confirm that the highest value (342MPa) corresponds to 0.75%wt of ZIF-67. On the contrary, the lowest results in both Figure 4.5 and Figure 4.6 were obtained at 1%wt.

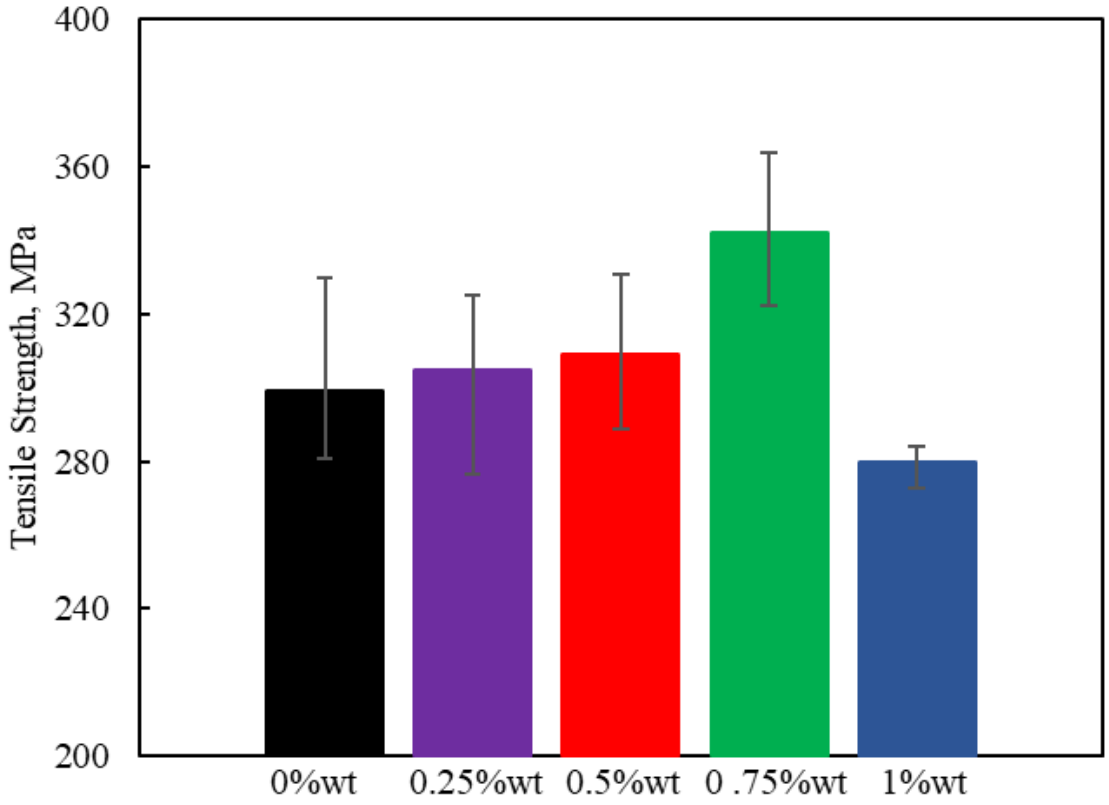

Figure 4.6: Maximum tensile stress values of 0 (Reference), 0.5, 0.75, and 1 wt% ZIF-67

Figure 4.7 summarizes the values of elastic modulus; the trend of the obtained values corresponds to information from previous studies. In other words, with the increase of concentration of ZIF-67 from 0%wt to 0.75%wt, Young's modulus values showed steady growth; however, further increase of concentration led to an insignificant result in contrast to the previous.

Non-monotonic pattern is observed amidst tensile strength and elastic modulus from 0%wt and 0.75%wt respectively. An increment of former values is followed by sudden drop when FRP was incorporated with 1%wt of ZIF-67, this trend is widely observed in nanocomposites, in other words, addition of excessive portion of nanomaterials is eligible for structure being defected, which in turn results in deterioration of tensile strength and elastic modulus results. Having conducted testings, the excessive amount being integrated in FRP is expected to be 1%wt of MOF. So, the optimal weight percentage of ZIF-67 for fiber-reinforced polymer is 0.75%wt. Obtained FRP data, the peak of the bar chart for ultimate tensile strength is in the

0.75 wt% ZIF-67 sample, and the strength of the 1.0 wt% sample reverts to baseline. This confirms that the optimum ZIF-67 content is at 0.75 wt%, and beyond this the benefit is lost. The more nanomaterials are added, the more chance of agglomeration phenomenon to be observed in the samples.

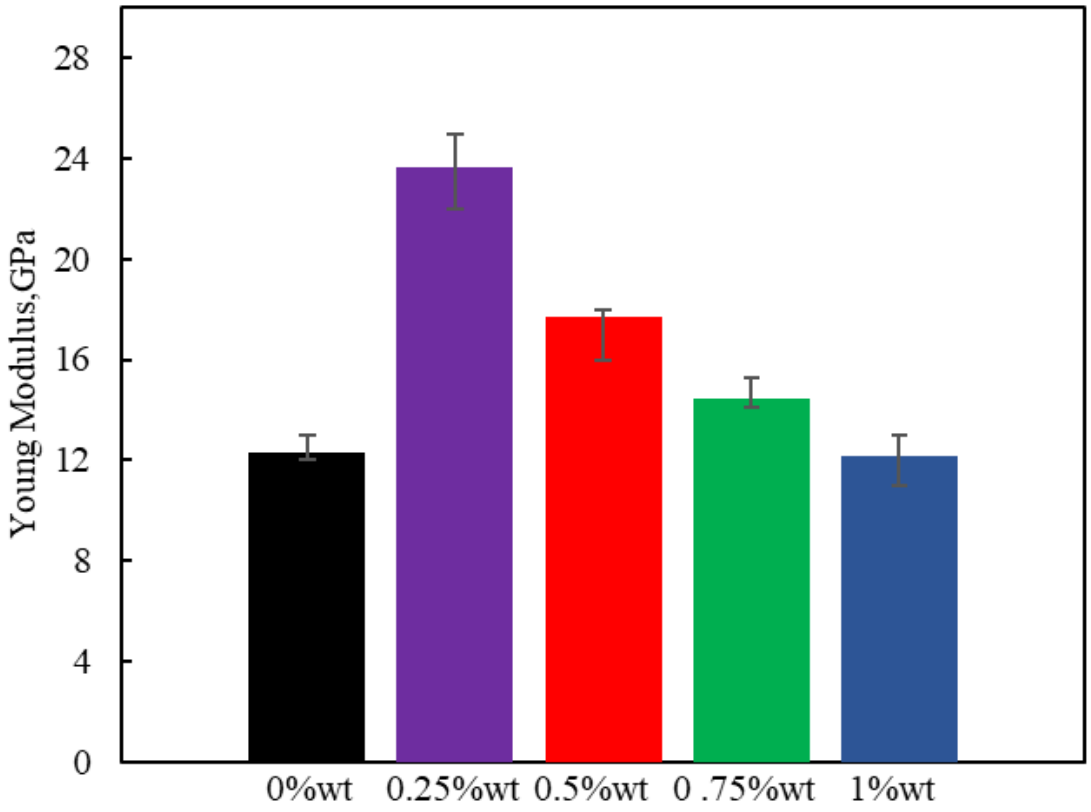

Figure 4.7: Young's modulus for FRP with different MOF fractions.

The observed trends can be potentially explained by the interfacial effects and poor ZIF-67 dispersion abilities. Low weight concentration of MOF is believed to be dispersed well augmenting contact area between carbon fiber, epoxy and ZIF-67. In result, the additional pathways for load transfer are being created, so that the rigid MOF particles and their surfaces can mechanically entangle with the epoxy chains, moreover, it can coat carbon surfaces to strengthen the matrix.

Nanoparticles are known for possessing strong van der Waals forces as well as for having a tendency to cluster. High weight concentrations of ZIF-67 start to interact, followed by further

clumping rather than being evenly distributed. Therefore, cracks initiate at these points, having an impact on load-transfer efficiency across the cluster-matrix boundary.

4.2.2 Three-Point Bending Testing

A Three-Point bending test was performed for the same combinations of FRP with ZIF-67. The results of this type of testing can be observed in Figure 4.8. The results are presented in the Load versus Displacement type of curve. However, the trend between the MOF concentrations can not be clearly observed, the overall pattern depicts an improvement in load capacity before being cracked in the middle. The highest load capacity corresponds to 1%wt (57N), while the lowest one is tied to 0.25%wt (27N). Integration of 0.5%wt and 0.75%wt into FRP is represented by the reinforcement of load-bearing capacity, since the displacement and force parameters increased proportionally compared to the 0%wt and 0.25%wt samples. Figure 4.8 illustrates the comparison of the Load-Bearing capacity of each of the FRP with different MOF fractions, and the trend in an increment of mechanical properties from 0%wt to 1%wt can be observed.

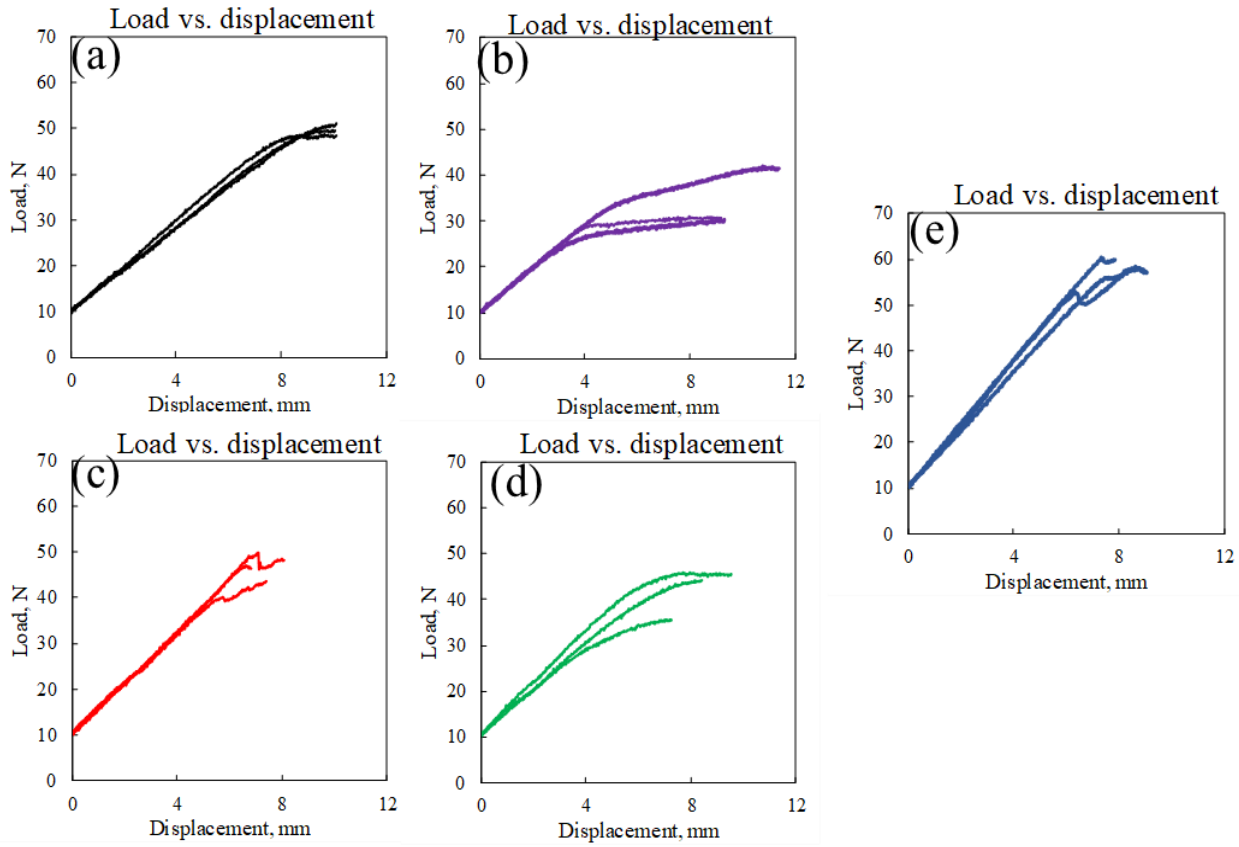

Figure 4.8: Three Point Bending Tests for FRP with MOF fractions: (a) 0%wt, (b) 0.25%wt, (c) 0.5%wt, (d) 0.75%wt, and (e) 1%wt.

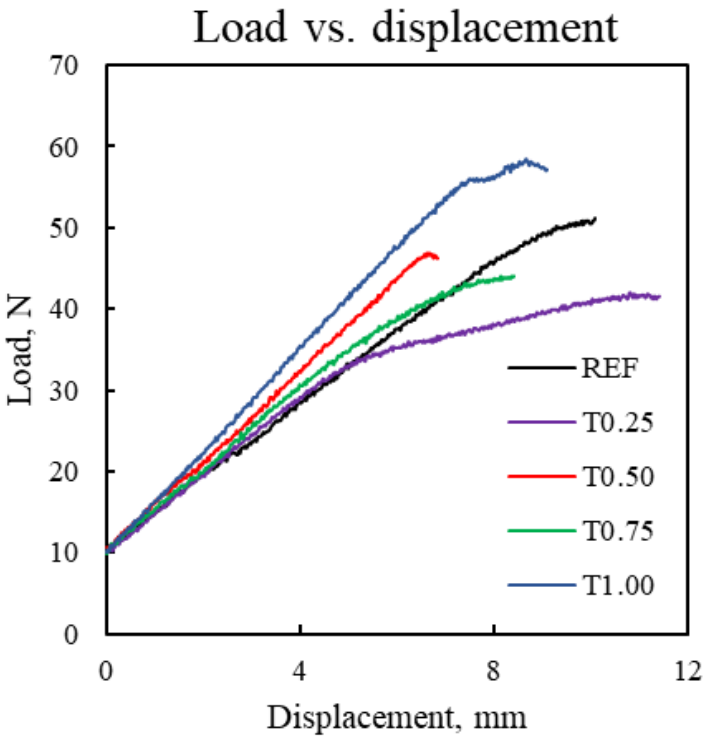

Figure 4.9: Three-point bending for FRP with MOF fractions.

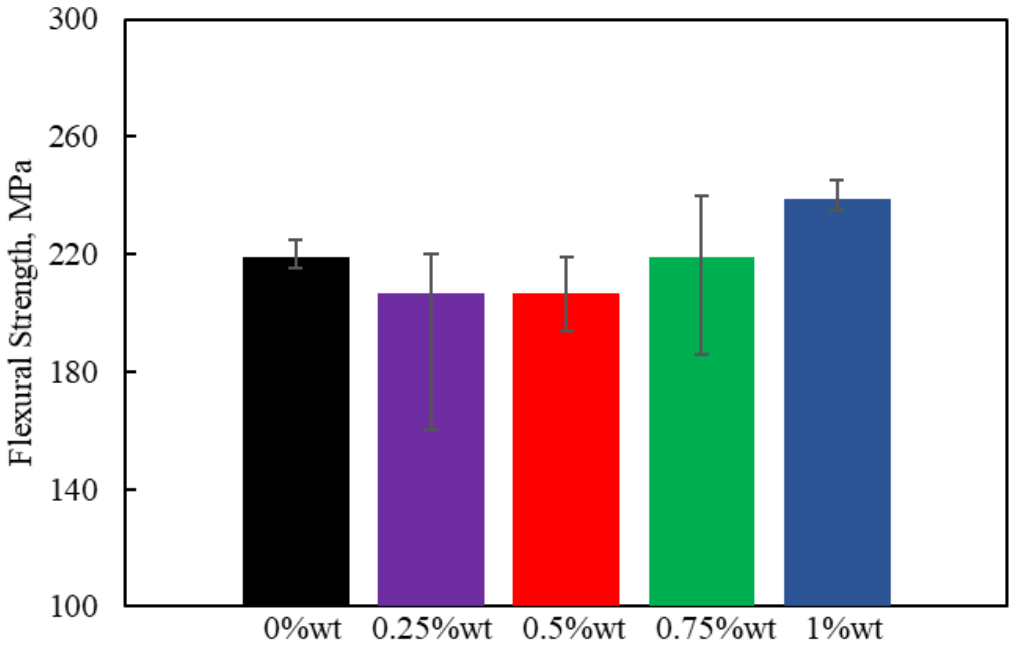

Figure 4.10: Flexural Strength for FRP with MOF fractions

Figure 4.10 shows a Flexural Strength obtained during Three Bending Testings, the highest value corresponds to the FRP with 1% (239MPa), while the lowest one is defined by 0.25% MOF fraction (206MPa). Overall, the Flexural Modulus shows an increase with the addition of ZIF-67 particles, in other words, improving the mechanical properties of composite.

The reinforcement occurs because of the rigid, crystalline structure of Metal-Organic Frameworks, which are believed to support the matrix of FRP. Moreover, porosity of MOFs is responsible for proper distribution of load by decreasing the local stress concentrations, which can result in premature failure of the sample. Therefore, the FRP incorporated with MOF becomes more resilient to be deformed under applied stress. Furthermore, the importance of molecular interactions of FRP integrated with MOF can not be neglected, since the adhesion is expected to be ameliorated, leading to improvement of interfacial bonding. Table 4.1 represents the summary of improvements of mechanical properties.

Table 4.1: Mechanical changes of FRP with different MOF fractions

FRP, %wt	Changes in Tensile strength	Changes in Flexural strength	Changes in Young's Modulus
0.25	+5%	+6.67%	+108%
0.50	+9.6%	+2.5%	+60%
0.75	+14.3%	+11.6%	+58%
1.00	+1.06%	+8.2%	-10.5%

4.3 Morphology of the Composite

The scanning electron microscope (SEM) representation of CFRPs with 0 wt% ZIF-67 after the tensile test, 0.5 wt% after the tensile test, and 1 wt% after the bending test are shown in Figures 4.11(a-d), 4.11(e-h), and 4.11(i-l), respectively. The differences in fracture behavior between the tensile test and the bending test can be observed, as in the former, the force was applied

unidirectionally, whereas in the latter, it was applied crosswise to the direction of carbon fiber orientation. The following figures will reveal more closely how the nano-MOF ZIF-67 influenced the fracture morphology, interfacial adhesion, and overall structural integrity of the final product.

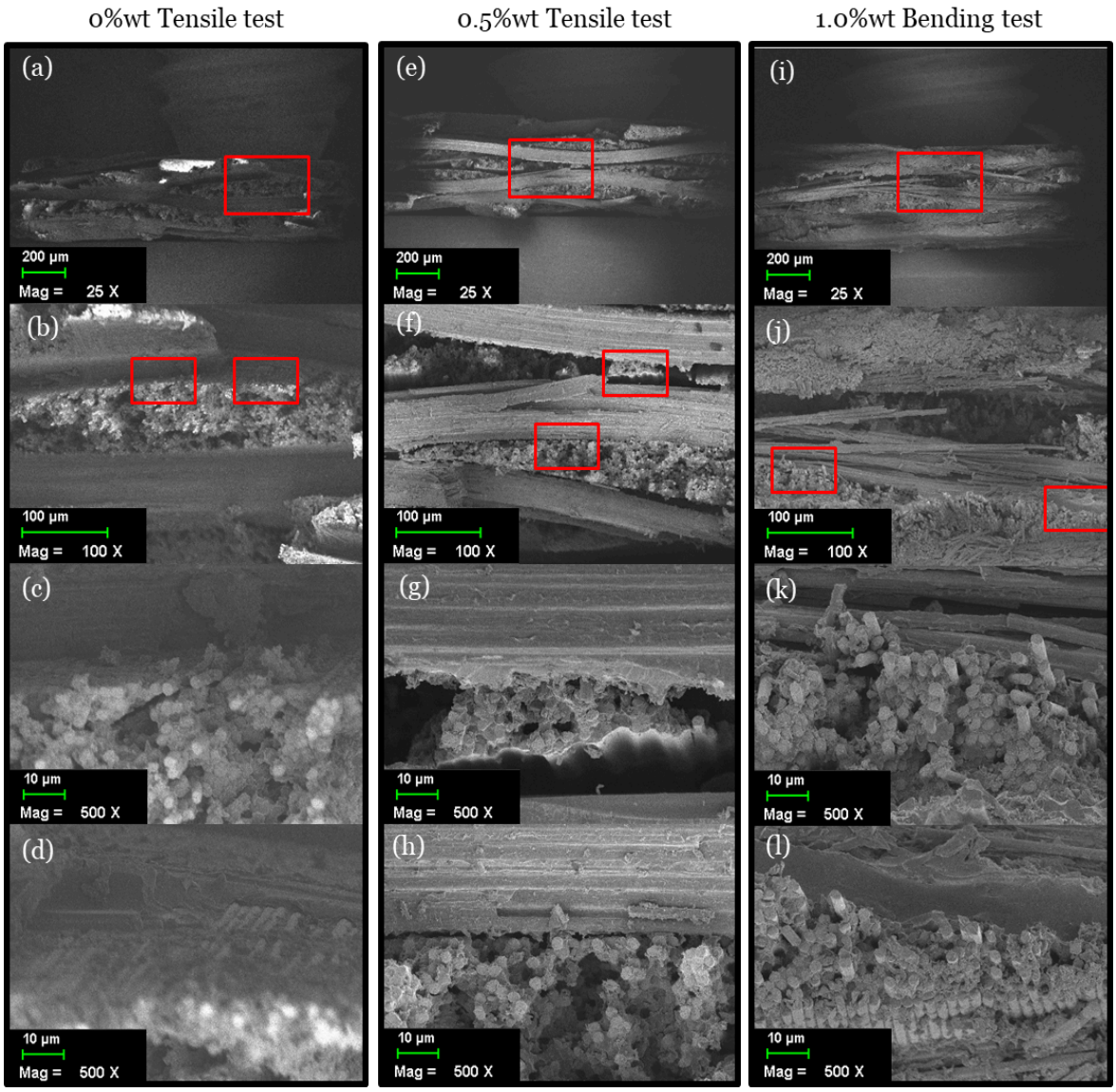

Figure 4.11: SEM images of (a–d) sample with 0 wt% ZIF-67 after tensile test, (e–h) sample with 0.5 wt% ZIF-67 after tensile, and (i–l) sample with 1 wt% ZIF-67 after the bending test.

In Figures 4.12 (a–d), higher-magnification SEM images of CFRP with 0 wt% MOF after the tensile test are presented. Starting from a magnification of 3000 X in Figure 4.12 (b), clear delamination of the fibers and the epoxy can be observed at the fracture surface. This

delamination indicates poor interfacial adhesion and reduced load transfer efficiency. These observations suggest that the incorporation of nano-MOFs is necessary to improve fiber-matrix bonding.

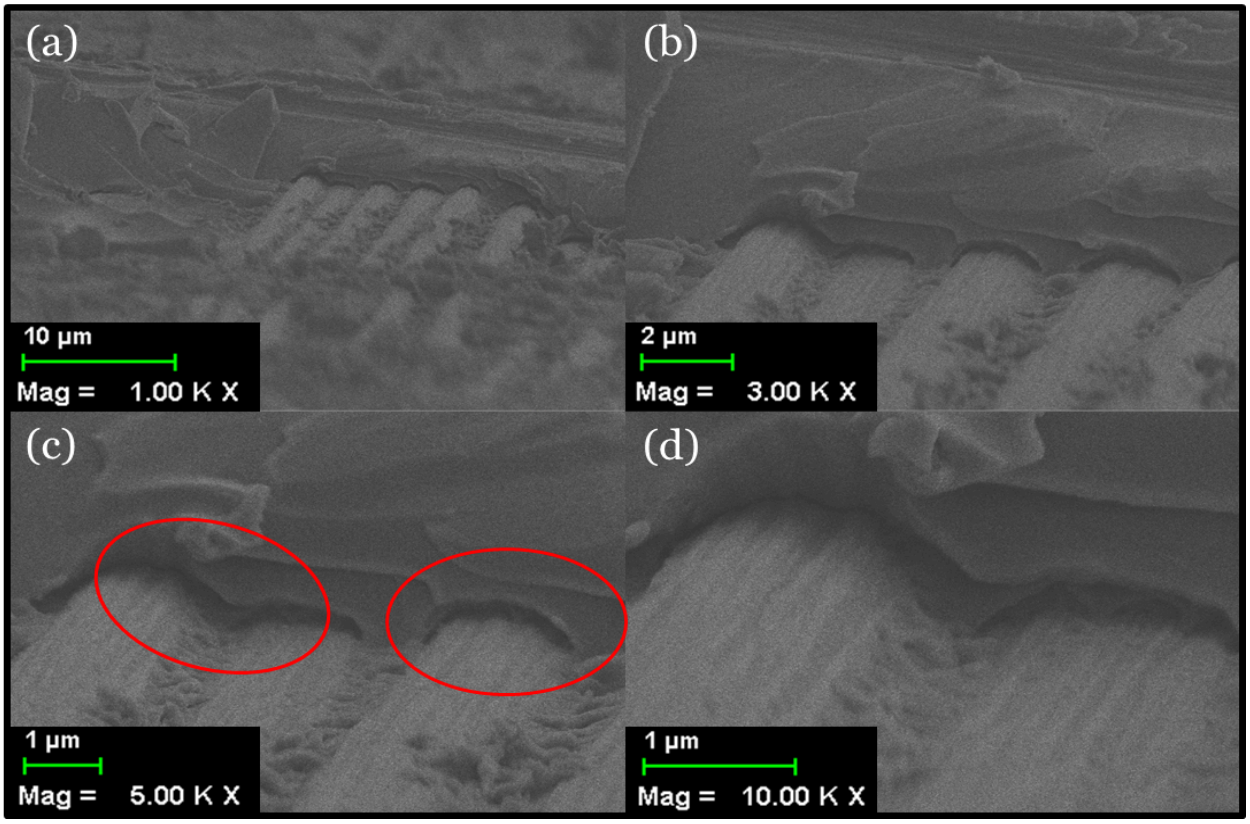

Figure 4.12: Higher-magnification SEM images of fracture for the sample with 0wt% ZIF-67 after the tensile test.

Figures 4.13 (a–b) and 4.14 (a–d) represent the fracture of the sample with 0.5 wt% MOF. In the areas highlighted with red lines, it is clearly visible how the fibers and matrix have interacted and bonded together. The way the fibers and the matrix are connected affects how the material breaks (fracture morphology), how well the fibers stick to the matrix (fiber-matrix adhesion), and how strong and damage-resistant the overall structure is (structural integrity). In this case, better connection between the carbon and matrix helps the material resist cracking and prevents layers from separating (delamination), making the composite tougher and stronger.

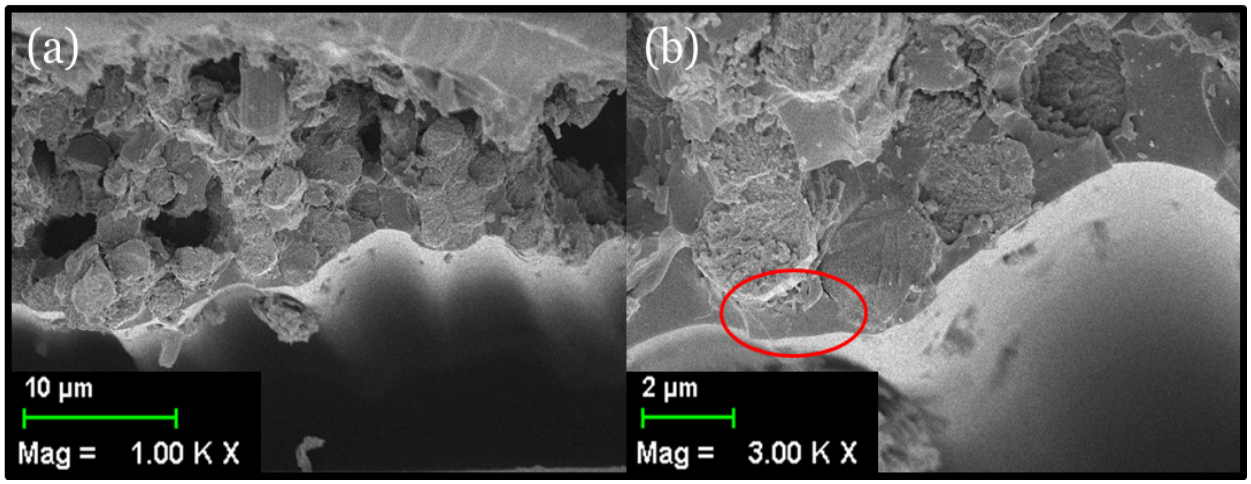

Figure 4.13: Higher-magnification SEM images of fracture for the sample with 0.5 wt% ZIF-67 after the tensile test (first region).

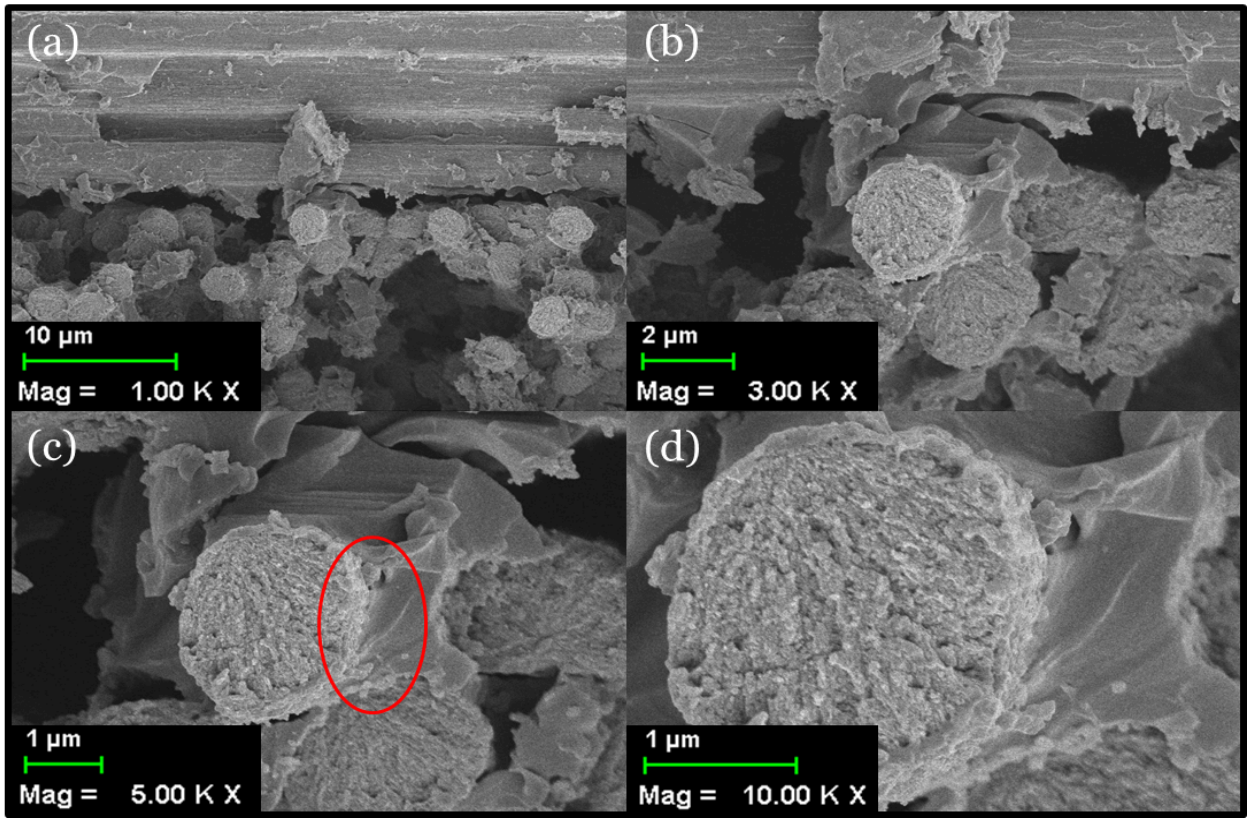

Figure 4.14: Higher-magnification SEM images of fracture surface for sample with 0.5 wt% ZIF-67 after the tensile test (second region).

For comparison, the fracture surfaces of the sample containing 1 wt% MOF after the bending test are shown in Figures 4.15 (a–d) and 4.16 (a-d). At higher magnification, a more uniform distribution of the matrix around the fibers can be observed, indicating further improvement in fiber-matrix interaction.

This enhanced interfacial adhesion reduces the likelihood of fiber pull-out and layer separation under bending stresses, and it is also critical for efficient load transfer. As a result, improved toughness and structural stability can be expected in the composite.

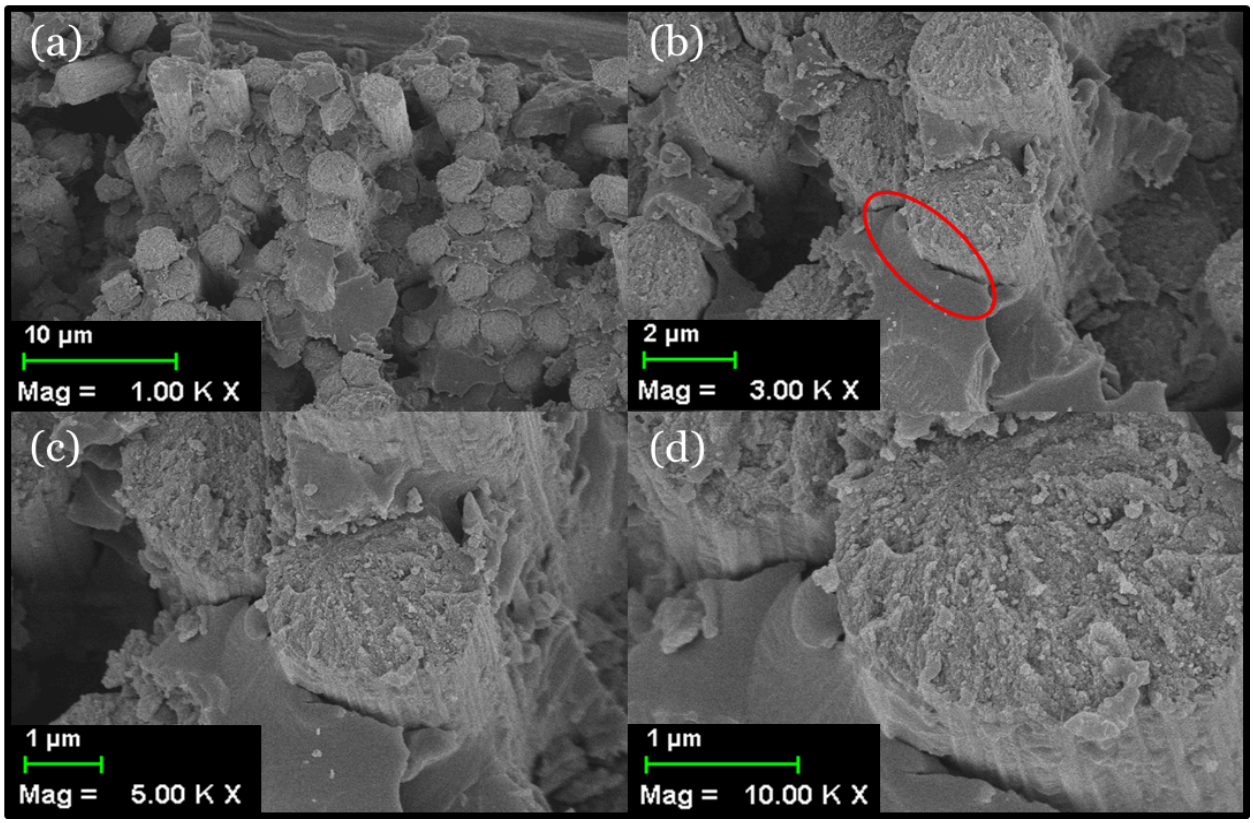

Figure 4.15: Higher-magnification SEM images of fracture for sample with 1.0 wt% ZIF-67 after the bending test (first region).

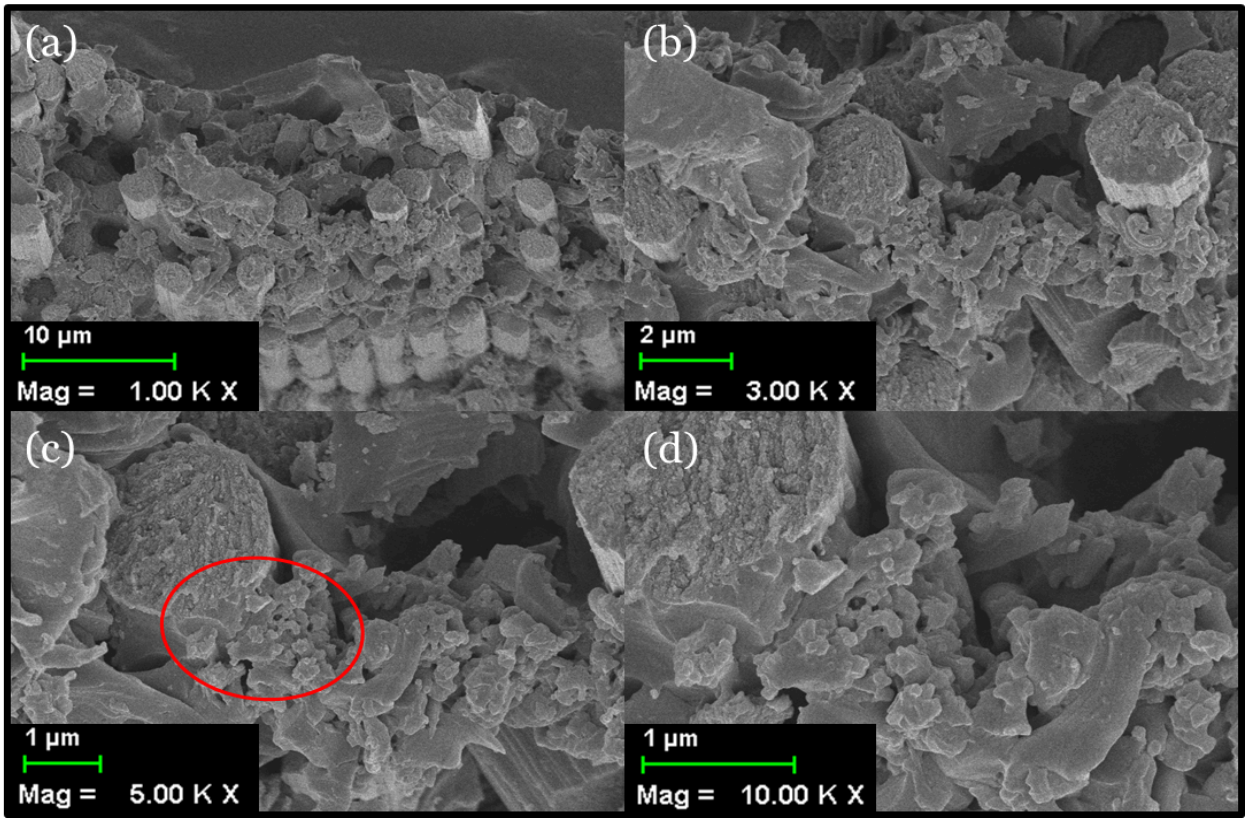

Figure 4.16: Higher-magnification SEM images of fracture for sample with 1.0 wt% ZIF-67 after the bending test (second region).

4.4 Future Recommendations

The research has demonstrated that even a small incorporation of ZIF-67 into FRP leads to significant enhancement of mechanical properties; however, there are still several avenues that remain unexplored, and future research is vital.

Firstly, dispersion techniques should be further developed in order to avoid the agglomeration of MOF particles, which was observed at higher concentrations. Such methods as high-shear mixing and in situ polymerization may be considered as appropriate ways of creating more homogeneous particle distribution, and as result, will create more consistent reinforcement and will diminish the stress concentration zones.

Secondly, the research was investigating only the mechanical properties of composites, however, thermal and environmental stability should also be taken into account, since it directly

affects the applicability of the final product. Therefore, it is recommended for future studies to include thermal degradation analysis as well as environmental exposure tests to evaluate durability under different conditions.

Thirdly, the scope of research can be changed from zeolitic group of MOF to other MOF structures such as MIL-101 or UiO-66. Alternative MOF structures could lend improved bonding, porosity or versatility of data.

Moreover, in order to assess energy dissipation and load-bearing behaviour in a proper way, mre mechanical testing can be conducted. Impact Fatigue data measurements can be considered as an example, because these tests are pivotal for describing cyclic and vibrational environments.

Finally, some feasibility studies can be conducted in order to evaluate the process of MOF integration into the FRP, and should the purported mechanical improvements outweigh its cost production, since the process of fabrication of single FRP is expensive enough. However, results of MOF incorporation showed that the cost production has to be optimized, due to a

ement in mechanical performance.

By addressing these issues, further research on distinct MOF-based nanomaterials can be made resulting in acceleration of its transition from laboratory innovation to practicum, by implementing it in high-performance materials in aerospace/automotive industries.

Chapter V

Conclusion

In this capstone project, nanosized ZIF-67 metal-organic frameworks (MOFs) were synthesized and incorporated into carbon fiber reinforced polymer (CFRP) composites in order to investigate their effect in terms of mechanical properties. The success of the synthesis of ZIF-67 was confirmed through 3 levels of characterization:

1) X-ray diffraction (XRD) revealed the high crystallinity and phase purity of ZIF-67.
2) Scanning electron microscopy (SEM) confirmed both morphological features of ZIF-67 uniform particle size distribution and porous structure.
3) Fourier-transform infrared spectroscopy (FTIR) identified characteristic vibrational modes.

In each case, the incorporation of ZIF-67 resulted in notable improvements in mechanical properties. Tensile testing demonstrated an increase of 14.3% in ultimate tensile strength and 17% in elastic modulus at an optimal MOF loading of 0.75 wt%. Flexural testing revealed a 11.6% enhancement in flexural strength under the same loading condition. However, at a higher concentration of 1 wt%, there was a significant decrease in tensile strength. Such deviation is associated with agglomeration of the particles, which leads to uneven reinforcement of samples and consequent limitation of strength gains. Besides, these issues can create local stresses, and ultimately, some form of delamination may develop between the layers.

Fractographic analysis by SEM provided detailed microstructural changes associated with MOF incorporation. The reference CFRP samples without MOF addition exhibited significant fiber pull-out, smooth fiber surfaces, and evident matrix cracking, which indicates poor interfacial adhesion. In contrast, the results for CFRP composites with 0.5 wt% of ZIF-67 demonstrated a roughened fracture morphology with matrix residues adhering to fiber surfaces. Such results clearly indicate enhanced fiber-matrix interfacial bonding. At 1 wt% loading, SEM images exhibited increased microvoid formation, fiber debonding, and signs of interfacial delamination, which in their turn indicate mechanical property deterioration.

5. Conclusion

Overall, obtained results clearly suggest that low concentrations of ZIF-67 can effectively improve the mechanical behavior of CFRP composites by enhancing interfacial adhesion and load transfer. For future studies, it is recommended to focus on refining dispersion techniques for MOFs in order to diminish agglomeration effects. Such techniques like in situ polymerization, high-shear mixing, and chemical surface modification may be considered as promising approaches to address this issue. Additionally, further investigation of alternative MOF structures outside the zeolitic group guarantees to expand the functional capabilities of MOF-reinforced polymer composites and to fully realize their application potential.

Bibliography

[1] Karataş, M. A., & Gökkaya, H. (2018). A review on machinability of carbon fiber reinforced polymer (CFRP) and glass fiber reinforced polymer (GFRP) composite materials. Defence Technology, 14(4), 318–326. https://doi.org/10.1016/j.dt.2018.02.001

[2] Kamarudin, S. H., Basri, M. S. M., Rayung, M., Abu, F., Ahmad, S., Norizan, M. N., Osman, S., Sarifuddin, N., Desa, M. S. Z. M., Abdullah, U. H., Tawakkal, I. S. M. A., & Abdullah, L. C. (2022). A Review on Natural Fiber Reinforced Polymer Composites (NFRPC) for Sustainable Industrial Applications. *Polymers*, *14*(17), 3698. https://doi.org/10.3390/polym14173698

[3] Rashid, A. B., Haque, M., Islam, S. M. M., & Labib, K. R. U. (2024). Nanotechnology-enhanced fiber-reinforced polymer composites: Recent advancements on processing techniques and applications. *Heliyon*, *10*(2), e24692. https://doi.org/10.1016/j.heliyon.2024.e24692

[4] Zheng H., Zhang W., Li B., Zhu J., Wang C., Song G., et al., "Recent advances of interphases in carbon fiber-reinforced polymer composites: A review," *Composites Part B: Engineering*, vol. 233, Jan. 2022, https://doi.org/10.1016/j.compositesb.2022.109639.

[5] Hafezeh Nabipour, Xin Wang, Lei Song, Yuan Hu. "Metal-organic frameworks for flame retardant polymers application: A critical review." *Composites Part A*, Volume 139, 2020, 106113. DOI: 10.1016/j.compositesa.2020.106113.

[6] Bibekananda De, Madhab Bera, Debashish Bhattacharjee, Bankim Chandra Ray, Subrata Mukherjee. "A comprehensive review on fiber-reinforced polymer composites: Raw materials to applications, recycling, and waste management." *Progress in Materials Science*, Volume 146, 2024, 101326. DOI: 10.1016/j.pmatsci.2024.101326.

[7] Fuentes, A., & Moore, P. (2009). Strength and fatigue of short glass fibre reinforced PA6 in hostile environments. *Composites Part B: Engineering, 40*(8), 735–741. https://doi.org/10.1016/j.compositesb.2009.05.003

[8] Darain, K., & Zia, A. (2015). The effect of width, multiple layers, and strength of FRP sheets on strength and ductility of strengthened reinforced concrete beams in flexure. *International Journal of Advanced Structures and Geotechnical Engineering, 4*(2), 76–84. Retrieved from https://www.researchgate.net/publication/277533525

[9] Rashid, A. B., & Hoque, M. E. (n.d.). Polymer nanocomposites for defense applications. In *Elsevier eBooks* (pp. 373–414). https://doi.org/10.1016/b978-0-12-824492-0.00015-5

[10] Demiroglu, S., Singaravelu, V., Seydibeyoğlu, M. Ö., Misra, M., & Mohanty, A. K. (2017). The use of nanotechnology for fibre-reinforced polymer composites. In *Elsevier eBooks* (pp. 277–297). https://doi.org/10.1016/b978-0-08-101871-2.00013-8

[11] Su, C., Wang, X., Ding, L., & Wu, Z. (2020). Enhancement of mechanical behavior of FRP composites modified by silica nanoparticles. *Construction and Building Materials*, *262*, 120769. https://doi.org/10.1016/j.conbuildmat.2020.120769

[12] De Cicco, D., Asaee, Z., & Taheri, F. (2017). Use of nanoparticles for enhancing the interlaminar properties of Fiber-Reinforced composites and adhesively bonded Joints—A Review. *Nanomaterials*, *7*(11), 360. https://doi.org/10.3390/nano7110360

[13] Phonthammachai N, Li X, Wong S, Chia H, Weei W. Fabrication of cfrp from high-performance clay/epoxy nanocomposite: preparation conditions, thermal-mechanical properties and interlaminar fracture characteristics. Compos-A: Appl Sci Manuf 2011;42(8):881–7. https://doi.org/10.1016/j.compositesa.2011.02.014.

[14] Tian Y, Zhang H, Zhang Z. Influence of nanoparticles on the interfacial properties of fiber-reinforced-epoxy composites. Compos-A: Appl Sci Manuf 2017;98: 1–8. https://doi.org/10.1016/j.compositesa.2017.03.007.

[15] Zhang X, Fan X, Yan C, Li H, Zhu Y, Li X, et al. Interfacial microstructure and properties of carbon fiber composites modified with graphene oxide. ACS Appl Mater Interfaces 2012;4(3):1543–52. https://doi.org/10.1021/am201757v.

[16] Qin W, Vautard F, Drzal LT, Yu J. Mechanical and electrical properties of carbon fiber composites with incorporation of graphene nanoplatelets at the fiber–matrix interphase. Compos B Eng 2015;69:335–41. https://doi.org/10.1016/j.compositesb.2014.10.014

[17] Pathak AK, Borah M, Gupta A, Yokozeki T, Dhakate SR. Improved mechanical properties of carbon fiber/graphene oxide-epoxy hybrid composites. Compos Sci Technol 2016;135:28–38. https://doi.org/10.1016/j.compscitech.2016.09.007.

[18] Kim M, Park YB, Okoli OI, Zhang C. Processing, characterization, and modeling of carbon nanotube-reinforced multiscale composites. Compos Sci Technol 2009;69(3–4):335–42. https://doi.org/10.1016/j.compscitech.2008.10.019.

[19] Lee JH, Rhee KY, Park SJ. Silane modification of carbon nanotubes and its effects on the material properties of carbon/CNT/epoxy three-phase composites. Compos-A: Appl Sci Manuf 2011;42(5):478–83. https://doi.org/10.1016/j.compositesa.2011.01.004.

[20] Duan, S., Dou, B., Lin, X., Zhao, S., Emori, W., Pan, J., Hu, H., & Xiao, H. (2021). Influence of active nanofiller ZIF-8 metal-organic framework (MOF) by microemulsion method on anticorrosion of epoxy coatings. *Colloids and Surfaces a Physicochemical and Engineering Aspects*, *624*, 126836. https://doi.org/10.1016/j.colsurfa.2021.126836

[21] Zhang, W., Taheri-Ledari, R., Saeidirad, M., Qazi, F. S., Kashtiaray, A., Ganjali, F., Tian, Y., & Maleki, A. (2022). Regulation of Porosity in MOFs: A review on tunable scaffolds and related effects and advances in different applications. *Journal of Environmental Chemical Engineering*, *10*(6), 108836. https://doi.org/10.1016/j.jece.2022.108836

[22] S. Ayyagari, M. Al-Haik, Y. Ren, A. Abbott, E.B. Trigg, B. Zheng, H. Koerner. "Metal organic frameworks modification of carbon fiber composite interface." *Composites Part B*, Volume 224, 2021, 109197. DOI: 10.1016/j.compositesb.2021.109197

[23] Al-Haik, M., Ayyagari, S., Ren, Y., Abbott, A., Zheng, B. Q., & Koerner, H. (2023). Hybrid Metal-Organic Frameworks/Carbon fibers reinforcements for additively manufactured composites. *Nanomaterials*, *13*(5), 944. https://doi.org/10.3390/nano13050944

[24] P.A. Sreekumar, Selvin P. Thomas, Jean Marc Saiter, Kuruvilla Joseph, G. Unnikrishnan, Sabu Thomas. "Effect of fiber surface modification on the mechanical and water absorption characteristics of sisal/polyester composites fabricated by resin transfer molding." *Composites Part A*, Volume 40, 2009, Pages 1777-1784. DOI: 10.1016/j.compositesa.2009.08.013

[25] Zulfiqar Ali, et al. "The Effect of Width, Multiple Layers, and Strength of FRP Sheets on Strength and Ductility of Strengthened Reinforced Concrete Beams in Flexure." *ResearchGate*. Accessed at Link

[26]A. Singh, S. P. Shamchi, C. Sguazzo, X. Yi, Z. Zhao, and P. M. G. P. Moreira, “Analysis of Mechanical Behavior of Multi-functional CFRP under Bending and DCB Mode-I Fracture,” *Procedia Structural Integrity*, vol. 28, pp. 2206–2217, Jan. 2020, https://doi.org/10.1016/j.prostr.2020.11.049

[27] Saeed, S., Bashir, R., Rehman, S. U., Nazir, M. T., ALOthman, Z. A., Muteb Aljuwayid, A., Abid, A., & Adnan, A. (2022). Synthesis and Characterization of ZIF-67 Mixed Matrix Nanobiocatalysis for CO2 Adsorption Performance. Frontiers in Bioengineering and Biotechnology, 10. https://doi.org/10.3389/fbioe.2022.891549

[28] Narimbi, J.; Balakrishnan, S.; Perova, T.S.; Dee, G.; Swiegers, G.F.; Gun’ko, Y.K. XRD and Spectroscopic Investigations of ZIF—Microchannel Glass Plates Composites. Materials 2023, 16, 2410. https://doi.org/10.3390/ma16062410

[29] S. A. Khan, M. E. Johnson, M. S. Kalan, A. R. Montoro Bustos, S. A. Rabb, I. H. Strenge, K. E. Murphy, and T. R. Croley, "Characterization of nanoparticles in silicon dioxide food additive," *Food Additives & Contaminants: Part A, Chemistry, Analysis, Control, Exposure & Risk Assessment*, vol. 41, no. 1, pp. 9–21, 2024. https://doi.org/10.1080/19440049.2023.2297420

[30] X. Shi, Y. Hu, H.-M. Meng, J. Yang, L. Qu, X.-B. Zhang, and Z. Li, "Red emissive carbon dots with dual targetability for imaging polarity in living cells," *Materials Letters*, vol. 264, p. 127582, Apr. 2020. https://doi.org/10.1016/j.matlet.2020.127582

[31] S. R. Maske, R. K. Prusty, and B. C. Ray, "Effect of MWCNT/Nanosilica reinforcement on the mechanical and thermal behaviour of polymer composite," *Materials Today: Proceedings*, vol. 62, no. 10, pp. 6087–6090, 2022. https://doi.org/10.1016/j.matpr.2022.04.1015

[32] ASTM International, Standard Test Method for Tensile Properties of Polymer Matrix Composite Materials, ASTM D3039/D3039M-08, West Conshohocken, PA, USA, 2008. https://store.astm.org/d3039_d3039m-08.html

[33] ASTM International, Standard Test Methods for Flexural Properties of Unreinforced and Reinforced Plastics and Electrical Insulating Materials, ASTM D790-17, West Conshohocken, PA, USA, 2017. https://store.astm.org/d0790-17.html